https://doi.org/10.1016/j.trc.2021.103366

Joint design of shared-bike and transit services in corridors

Xiaoling Luo [a], Weihua Gu [b], Wenbo Fan [a *]

[a] Department of Traffic Engineering, School of Transportation and Logistics, Southwest Jiaotong University, Chengdu, China; [b] Department of Electrical Engineering, The Hong Kong Polytechnic University, Hung Hom, Kowloon, Hong Kong SAR, China;

[*] Corresponding author, Email: wbfan@swjtu.edu.cn

Abstract

The prevalence of shared bikes in many cities is a double-edged sword to the local mass transit services. Some transit patrons may switch to cycling, causing declines in the transit ridership. Others may benefit from using bikes instead of walking to access transit. The complicated interactions between the two modes entail the necessity of designing them jointly. Unfortunately, the literature has focused on either the design of a single mode or joint designs idealized by assuming a uniform demand pattern. The latter class of works has limited practical values.

This paper develops a continuum approximation (CA) model for optimizing the hybrid design of shared-bike and transit services in a corridor under spatially heterogeneous demand patterns. The model minimizes the generalized system cost considering various route options that patrons can choose from, including transit routes with walking or biking access and bike-only routes. The methodological challenges that arise due to patrons' route choices in the heterogeneous operating environment are overcome by incorporating a route assignment model into the CA modeling framework. We propose a bi-level algorithm to solve the model, where the upper level optimizes the hybrid design by exploiting some analytical properties of the CA model, and the lower level calculates the route assignment equilibrium.

Numerical experiments show that the optimal hybrid design outperforms the conventional transit design for a wide range of operating conditions. The cost saving can be over 20%. Under certain conditions, the hybrid design can even reduce the total operating cost, making bike-sharing profitable for transit agencies. The practical applicability of our model is demonstrated via a case study of a real bus line in Chengdu, China.

Keywords: bike-sharing; transit corridors; continuum approximation; heterogeneous demand; route assignment

1. Introduction

As an individual travel mode, bike-sharing bears more than the benefits of cycling, e.g., the convenience, affordability, and healthy and environmental merits. It also exhibits new appealing elements, e.g., the relief of bike ownership (Shaheen et al., 2010). As a result, bike-sharing systems have been widespread in over 1,000 cities worldwide (Wikipedia, 2019). Recent reports show that 51 million trips were taken

on shared bikes in the U.S. in 2018 (NACTO, 2018). In China, that number even reached 25 billion (People's Daily, 2018).

The success of bike-sharing is accompanied by mixed impacts on public transportation systems. Metro and subway systems are generally believed to benefit from the shared bikes. For instance, Ma et al. (2015) reported that a 10% increase of shared-bike rides led to a 2.8% increase in the Metrorail ridership in Washington, D.C. Graehler Jr. et al. (2019) revealed from the data of 22 major U.S. cities that a 4.2-6.9% increase in rail transit ridership could be attributed to bike-sharing programs. For bus transit, however, bike-sharing appears to be more of a competitor than a feeder mode in European and North American cities. For example, empirical studies of those cities accused bike-sharing of creating a 1-3% decrease in bus ridership (e.g., Parkes et al., 2013; Campbell and Brakewood, 2017; Graehler Jr. et al., 2019). On the other hand, studies of Chinese cities spoke to the opposite. For example, Ma et al. (2019) found that each shared bike in Chengdu brought in 4.23 additional daily bus trips on weekdays, albeit together with a reduction of 0.56 daily bus trips on weekends.

The empirical evidence shows that shared bikes and transit interact in a rather complicated way. However, proper long-term planning can render more synergistic interactions between the two modes (Singleton and Clifton, 2014). Efforts to integrate the two modes have been attempted in practice. These include the deployment of bike docking stations at transit stops (Martens, 2004; Rietveld, 2000) and launches of new bike-sharing systems directly operated by transit agencies (e.g., Call a Bike, 2019; Metro Bike Share, 2019).

Research works are ample in this realm too. For example, some focused on the bike docking-station location problem where existing transit stops were treated as candidate locations (Lin and Yang, 2011; García-Palomares et al., 2012; Lin et al., 2013; Conrow et al., 2018). Others examined the bike-sharing network design problem, considering patrons' mode choice between biking and an existing transit system (Chow and Sayarshad, 2014; Tavassoli and Tamannaei, 2020). On the other hand, transit system design problems given pre-existing shared bikes were also explored (e.g., Liu et al., 2019). Regrettably, all the above-cited works assumed either the transit network or the bike-sharing system is fixed. As a result, the joint design of the two systems has largely gone unreported.[1]

To our best knowledge, the first work on the optimal joint design of bike-sharing and transit services is Wu et al. (2020), where the shared bikes were used as feeders to the transit service. Analytical models were developed to optimize bike station density, transit line spacing, and transit headways. The work revealed that, in addition to reducing transit patrons' travel time, the joint design could even save the agency's operating cost under certain conditions. The overall system cost saving can be above 10% as compared to an optimal conventional transit system without shared bikes. The work was later

[1] Models were also developed for optimizing shared-bike operations. Examples include the bike deployment problem at docking stations (Shu et al., 2013; Tang et al., 2018), the docking-station sizing problem (Freund et al., 2017), and the bike rebalancing problem (Pal and Zhang, 2017). They mainly focused on an isolated bike-sharing system, and thus are not closely related to the topic of this paper.

extended to incorporate the option of completing a trip by bike only (Li et al., 2020). Nevertheless, these two studies are limited in that they only produced idealized, homogeneous network structures under uniform demand. They thus overlooked the modeling complexities that arise due to realistic, spatially heterogeneous demand patterns. Consequently, they failed to unveil how the optimal design varies with demand over space. Also, their models cannot be applied to design real-world systems.

There are two classes of methods for addressing demand heterogeneity. The first class of methods relies on discrete models that use numerous parameters and variables to represent spatially heterogeneous demand and design features (e.g., Szeto and Wu, 2011; Nayeem et al., 2014). Due to the complexity of those models, they were often applied to solve problems of limited sizes. Metaheuristic methods (e.g., genetic algorithm) were commonly used to find solutions in a reasonable runtime. The second class of methods employs the so-called "continuum approximation (CA)" technique, in which the heterogeneous demand density and design variables (e.g., stop spacing or density) are represented by continuous functions of spatial coordinates (e.g., Wirasinghe and Ghoneim, 1981). Efficient solution algorithms and even closed-form solutions can be developed thanks to the parsimony of these CA models. However, the formulation and solution of these models are more challenging than analytical models developed under the uniform demand assumption (e.g., Daganzo, 2010; Gu et al., 2016; Wu et al., 2020). For example, CA models were often solved by exploiting the local decomposition property. With this property, the optimization problem can be decomposed by spatial coordinates into subproblems, each containing a handful of scalar decision variables only (Chen et al., 2015). Unfortunately, many transit network design problems do not exhibit the local decomposition property, especially for multimodal transit systems where patrons distribute themselves among different modes and routes.

In light of the above, we propose a CA model to optimize the hybrid design of shared bikes and transit service in a corridor under heterogeneous demand. The design variables include the spatially varying densities of bike stations and transit stops and the transit service headway. We choose to model a corridor instead of a city-wide network because, to our best knowledge, the present mathematical tools for spatially heterogeneous transit network design are highly limited. Some previous CA models in this realm can only be applied to special demand patterns, e.g., rotationally symmetric demand that varies along radial lines only (Badia et al., 2014; Chen et al., 2015; Luo and Nie, 2019, 2020a). Others use special transit network layouts, e.g., grid-shaped networks where the line spacings were constrained by the power-of-two rule (Ouyang et al., 2014; Chen et al., 2018). The network structure used in the latter-cited works also requires some patrons to make unreasonably many (three or more) transfers in their journeys. On the other hand, CA methods for transit corridor design do not impose stringent restrictions on demand patterns or line layout (Wirasinghe and Ghoneim, 1981; Medina et al., 2013; Luo et al., 2020; Mei et al., 2021). Modeling a corridor instead of a city-wide network allows us to focus our efforts on tackling the challenges that arise due to the complicated interactions between the

105 transit and shared bikes. To our knowledge, these challenges have not been appropriately addressed in the literature under a heterogeneous operating environment.

To better understand the methodological challenges, note that patrons' route options in a hybrid system include transit routes accessed by walking, transit routes accessed by biking, and bike-only routes. Patrons' costs (mainly travel times) and some critical operating features (e.g., the patron flow 110 on each mode, which dictates the numbers of transit vehicles or bikes needed) depend heavily on their route choices. On the other hand, a patron's route choice hinges upon the route trip costs *under a given design*. Moreover, the probability of choosing a specific route depends on trip ODs and is also heterogeneous along the corridor. The latter adds a significant amount of complexity to the problem. To confront these challenges, we develop patrons' route choices in two steps: Step 1 identifies the best 115 access and egress modes to transit between cycling and walking using the "critical distance" concept borrowed from Wu et al. (2020); and Step 2 determines the choice of an arbitrary patron between the best transit-dominated route and the bike-only option by comparing their costs. Details of this novel route assignment model can be found in Sections 3.1 and 3.2. Cost models and the optimization formulation are furnished in Sections 3.3-3.5.

120 Regarding the solution approach, although the original problem involving route choice is not decomposable, we find that the model can be decomposed by the space coordinate if route assignment is fixed. Furthermore, analytical properties regarding the optimal solution can be derived for the decomposed model. Built upon these properties, we develop a bi-level heuristic algorithm that optimizes the system design and determines route assignment separately and iteratively. Details of the 125 solution approach can be found in Section 4.

Our extensive numerical experiments unveil valuable insights into cause-and-effect relations between key operating factors and the optimal design. The practical applicability of our model is verified via a case study of a real-world bus corridor in Chengdu, China. Details are offered in Section 5. Finally, Section 6 concludes the paper by summarizing its contributions and potential extensions.

130 We start by presenting the modeling framework and key assumptions in the next section.

2. Modeling framework

For the convenience of readers, notations used in this paper are summarized in Appendix A.

135 2.1. Layout

Consider an idealized transit (bus or metro) corridor with a length of L (km), as shown in Figure 1. The transit service is characterized by the service headway, h (hour), and the stop density, $\delta_t(x)$ (stops/km), which varies with location $x \in [0, L]$. Also deployed in the corridor are shared bikes, which dwell in

stations with or without docks.[2] The density of these bike stations is denoted $\delta_b(x)$ (stations/km), $x \in [0, L]$. To facilitate transfers between transit vehicles and shared bikes, we specify that each transit stop is coupled with a bike station, which implies $\delta_b(x) \geq \delta_t(x), x \in [0, L]$.

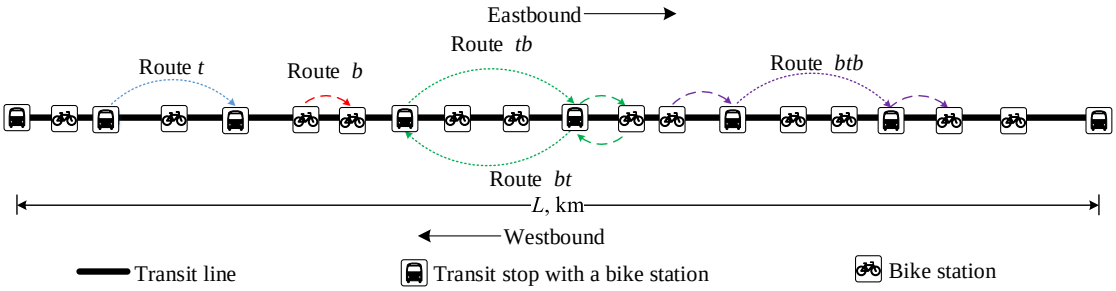

Figure 1. A transit corridor served by shared bikes.

2.2. Major assumptions

To facilitate the model formulation, we make the following assumptions, which were also commonly adopted in many previous CA studies (e.g., Murray, 2003; Estrada et al., 2011; Medina et al., 2013).

Assumption 1. The distribution of transit demand is spatially continuous and *slow-varying*, and time-invariant during the study period. The hourly demand density, $\lambda(x, y)$ (trips/km^2/h), is expressed as a function of trip origin and destination locations, x and $y \in [0, L]$.[3] Denote $\beta \in [0,1]$ as the fixed able-bodied patron ratio. For each OD pair (x, y), $\beta \cdot \lambda(x, y)$ is the demand density of *able-bodied patrons*, i.e., those who can ride bikes; $(1 - \beta) \cdot \lambda(x, y)$ is the demand density of non-able-bodied patrons who will always choose walking to access and egress transit. All patrons are identical regarding their social-economic characteristics. (For example, their value of time, VOT, is a constant.)

Assumption 2. Transit stops and bike stations can be located at any point in the corridor. Fine-tuning can be made to account for realistic location constraints, e.g., junctions and ramps (Estrada et al., 2011; Luo et al., 2020).

Assumption 3. The bike-sharing system implements a distance-based fee regime (Wu et al., 2020). The transit agency charges a flat fare for each trip.

We consider five types of routes in the hybrid system, as illustrated in Figure 1, which are denoted by $I \in \{t, b, bt, tb, btb\}$. Route t indicates that a patron walks to the nearest transit stop, takes transit to the closest stop to her destination, and walks to the destination. In route b, a patron finishes her trip by bike only. Routes tb, bt, and btb are intermodal routes where shared bikes serve as a feeder mode to the transit line. Particularly, routes tb and bt entail a shared bike to serve the last- and first-mile trip segments, respectively, while route btb uses shared bikes at both ends of a trip.

[2] Bike docking stations are common in the U.S., Canada, and the Netherlands, while dock-less bike stations are popular in China.
[3] In practice, a surveyed OD matrix can be converted to a continuous demand density function via interpolation.

Assumption 4. Between the bike-only route b and the route options involving transit, an able-bodied patron always chooses the one with the minimum expected travel cost. Among transit route options, the able-bodied patron chooses the access/egress mode between walking and cycling by comparing their access/egress times to the nearest transit stop. The patron always walks to or from the closest bike station to pick up or return a shared bike.

Assumption 5. Transit vehicles operate in a deterministic manner without considering random disturbances in their schedules. Transit patrons arrive at stops randomly without consulting the service schedule.

3. Models

We first present the route travel cost models in Section 3.1. Based on these models, the route demand assignment model is developed in Section 3.2. Sections 3.3 and 3.4 formulate models for patrons' and agencies' costs, respectively. The optimization problem is formulated in Section 3.5. For simplicity, Sections 3.1-3.4 present models for the eastbound travel direction only since models for the westbound direction are the same. The subscript indicating travel direction is omitted in these sections.

3.1. Route travel costs

We first introduce the following result regarding patrons' access/egress mode choice, given that a transit-dominated route (i.e., not bike-only) is selected.

Proposition 1. There exists a critical distance[4], $d_{ck}(x) \in \left(0, \frac{1}{2\delta_t(x)}\right]$ for any $x \in [0, L]$, such that if an able-bodied patron's access or egress distance, d, satisfies $d \leq d_{ck}(x)$, she will choose to walk to or from the transit stop; otherwise, she will choose to ride a shared bike. Figure 2 illustrates the zones delineated by $d_{ck}(x)$.

Proof of Proposition 1 and the derivation of $d_{ck}(x)$ are relegated to Appendix B.

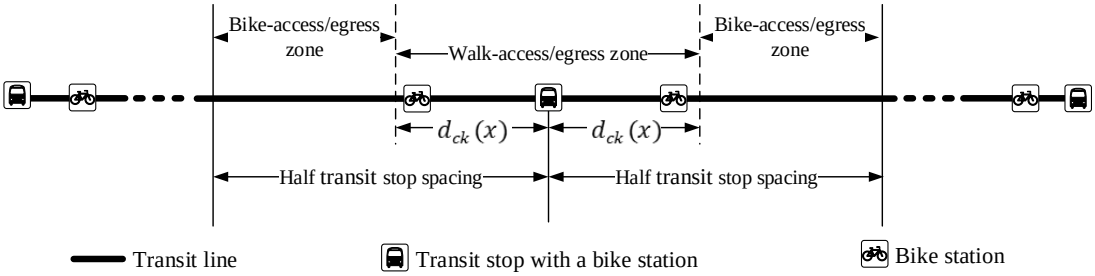

Figure 2. Walk- and bike-access/egress zones.

Following Proposition 1, the expected travel cost of route $I \in \{t, b, bt, tb, btb\}$ from point x to point y, $T_I(x, y)$, is formulated by:

$$T_t(x,y) = \kappa_t(x) + \kappa_t(y) + \frac{h}{2} + \int_x^y \frac{1}{V_t(u)} du + \frac{\varphi_t}{\mu}, \quad (1a)$$

[4] Similar concepts were also used in Wu et al. (2020) and Chen and Nie (2017).

$$T_b(x,y) = \kappa_b(x) + \kappa_b(y) + t_{pu} + t_{do} + \frac{|x-y|}{v_b} + \frac{\varphi_k(d_b(x,y))}{\mu}, \quad (1b)$$

$$T_{bt}(x,y) = \kappa_b(x) + \kappa_t(y) + \frac{h}{2} + \int_x^y \frac{1}{V_t(u)} du + f(x) + t_{pu} + t_{do} + \frac{\varphi_k(d_a(x))+\varphi_t}{\mu} + \xi_{b\to t}, \quad (1c)$$

$$T_{tb}(x,y) = \kappa_t(x) + \kappa_b(y) + \frac{h}{2} + \int_x^y \frac{1}{V_t(u)} du + f(y) + t_{pu} + t_{do} + \frac{\varphi_k(d_a(y))+\varphi_t}{\mu} + \xi_{t\to b}, \quad (1d)$$

$$T_{btb}(x,y) = \kappa_b(x) + \kappa_b(y) + \frac{h}{2} + \int_x^y \frac{1}{V_t(u)} du + f(x) + f(y) + 2\left(t_{pu} + t_{do}\right) + \frac{\varphi_k(d_a(x))+\varphi_k(d_a(y))+\varphi_t}{\mu} + \xi_{b\to t} + \xi_{t\to b}, \quad (1e)$$

where each travel time function consists of five parts: (i) the walking times to and from transit stops or bike stations; (ii) the waiting delay for transit vehicles and the pick-up/drop-off time loss for bikes; (iii) the transit and bike riding times; (iv) the service fare and fees; and (v) the transfer penalties (if an intermodal route is taken). They are explained as follows:

(i) The $\kappa_t(u)$ and $\kappa_b(u)$ ($u = x$ or y) in (1a-e) are the average walking time to/from the nearest transit stop and bike station, respectively. They are estimated by: $\kappa_t(u) = \frac{d_{ck}(u)}{2v_w}$ for able-bodied patrons and $\frac{1}{4v_w\delta_t(u)}$ for non-able-bodied ones; and $\kappa_b(u) = \frac{1}{4v_w\delta_b(u)}$, where v_w (km/h) is the walking speed.

(ii) The $\frac{h}{2}$ in (1a, 1c-e) is the average wait time for the next arriving transit vehicle, thanks to Assumption 5 in Section 2.2. The t_{pu} and t_{do} (h) in (1b-e) are the lost times for picking up and returning a bike at a bike station, respectively.

(iii) The riding distance by transit for route types t, bt, tb, and btb, and by bike for route type b, is approximated by $|x-y|$.[5] Thus, $\int_x^y \frac{1}{V_t(u)} du$ and $\frac{|x-y|}{v_b}$ yield the transit riding time for transit-dominated routes and the bike riding time for route type b, respectively, where $V_t(u)$ is the commercial transit speed at location u, and v_b (km/h) the average bike riding speed. The $V_t(u)$ satisfies $\frac{1}{V_t(u)} = \frac{1}{v_t} + \tau^o\delta_t(u) + \max\left(\tau^b B_t(u), \tau^a A_t(u)\right)h$, where v_t (km/h) is the transit cruise speed; τ^o (h) the fixed delay per stop due to vehicle acceleration, deceleration, and doors opening and closing; τ^b and τ^a (h) the delays per boarding and alighting patron, respectively;[6] and $B_t(u)$ and $A_t(u)$ the numbers of boarding and alighting patrons per km per hour in the vicinity of u.

For route types bt, tb, and btb, the access/egress travel time *by bike* should also be included. We denote $f(u)$ as the approximate average access or egress time by bike for an able-bodied patron

[5] Even under the heterogeneous demand, this approximation is good if the average trip length is much larger than the spacings between consecutive transit stops and bike stations. This is because a patron always walks to the nearest transit stop or bike station, which is located either upstream or downstream of her origin/destination with on average equal probabilities. The approximation error in our model is examined in Section 5.2.

[6] We assume that each transit vehicle operates two doors for boarding and alighting separately.

originated from or destined for u. We have $f(u) = \frac{1}{2}\left(\frac{1}{2\delta_t(u)} + d_{ck}(u)\right)\frac{1}{v_b}$, since $\frac{1}{2}\left(\frac{1}{2\delta_t(u)} + d_{ck}(u)\right)$ is the approximate average bike-riding distance in each access/egress segment; see Figure 2.

(iv) The φ_t (\$) and $\varphi_k(d)$ (\$) denote the flat transit fare and the distance-based bike rental fee, where d is the bike trip distance. Here we set $\varphi_k(d)$ as a linear function of trip distance d:

$$\varphi_k(d) = \varphi_k^1 d + \varphi_k^0, \tag{2}$$

where φ_k^0 (\$) and φ_k^1 (\$/km) are the fixed fee rate and the fee rate per km, respectively. For route type b, the cycling distance is $d_b(x, y) = |x - y|$; for access and egress segments by bike, the cycling distances are $d_a(x)$ and $d_a(y)$, respectively, where $d_a(u) = \frac{1}{2}\left(\frac{1}{2\delta_t(u)} + d_{ck}(u)\right)$. The fare and fees are divided by the VOT, μ (\$/h), to be converted into equivalents in hours.

(v) The $\xi_{b\to t}$ and $\xi_{t\to b}$ (h) are transfer penalties between bike and transit.

3.2. Route assignment

Following Assumptions 1 and 4 in Section 2.2, among the able-bodied demand, let $\lambda_I(x, y)$ be the density of trips taking route $I \in \{t, b, bt, tb, btb\}$ from origin x to destination y. The $\lambda_I(x, y)$ can be estimated by the product of the total able-bodied demand density and the route choice probability, $\mathcal{P}_I(x, y)$, i.e.,

$$\lambda_I(x, y) = \beta\lambda(x, y)\mathcal{P}_I(x, y), I \in \{t, b, bt, tb, btb\}. \tag{3}$$

We use a deterministic route choice model to develop $\mathcal{P}_I(x, y)$ in two steps. Models following a similar logic but developed under the uniform demand pattern were also found in Fan et al. (2018) and Luo and Nie (2020b). In the first step, we ignore the bike-only route type b, and divide all the able-bodied patrons into four classes according to the proximity of their ODs to transit stops. A specific route option among $\{t, bt, tb, btb\}$ will be selected as the best transit-dominated route in each class. To develop the probability that an arbitrary OD (x, y) falls in each trip class, we define $H(u) \in [0,1]$ as the probability that location $u \in [0, L]$ falls in a walk-access/egress zone. From Proposition 1, we have $H(u) = \frac{2d_{ck}(u)}{1/\delta_t(u)} = 2d_{ck}(u)\delta_t(u)$.[7] Therefore, the probability that an able-bodied trip (x, y) falls in the class where route t is preferred over routes tb, bt, and btb is $H(x)H(y)$. Similarly, the probabilities that (x, y) falls in classes where route bt, tb, and btb are respectively preferred over the other three options are: $\big(1 - H(x)\big)H(y)$, $H(x)\big(1 - H(y)\big)$, and $\big(1 - H(x)\big)\big(1 - H(y)\big)$.

[7] Note that these are approximations when the demand density varies spatially. Our slow-varying demand assumption (Assumption 1 in Section 2.2) ensures that the approximation errors would be small. This is later verified in Section 5.2. Similar approximations can also be found in previous studies, e.g., Newell (1971), Wirasinghe and Ghoneim (1981), Ouyang and Daganzo (2006), Ouyang et al. (2014), Luo and Nie (2020a), and Mei et al. (2021).

In the second step, we determine $\mathcal{P}_I(x,y)$ for $I \in \{t, b, bt, tb, btb\}$ by comparing the travel costs of route option b and an able-bodied patron's best transit-dominated route for each of the four classes of patrons. Specifically,

$$\mathcal{P}_t(x,y) = H(x)H(y)Q_t(x,y), \tag{4a}$$

$$\mathcal{P}_{bt}(x,y) = \big(1 - H(x)\big)\, H(y)Q_{bt}(x,y), \tag{4b}$$

$$\mathcal{P}_{tb}(x,y) = H(x)\big(1 - H(y)\big)Q_{tb}(x,y), \tag{4c}$$

$$\mathcal{P}_{btb}(x,y) = \big(1 - H(x)\big)\big(1 - H(y)\big)Q_{btb}(x,y), \tag{4d}$$

$$\mathcal{P}_b(x,y) = 1 - \textstyle\sum_{I\in\{t,bt,tb,btb\}} P_I(x,y), \tag{4e}$$

where $Q_I(x,y)$ ($I \in \{t, bt, tb, btb\}$) is a binary variable indicating whether route I has a lower travel cost than route b. It is expressed by:

$$Q_I(x,y) = \begin{cases} 1 & T_b(x,y) > T_I(x,y) \\ 0 & \text{otherwise} \end{cases}, I \in \{t, bt, tb, btb\}, \tag{5}$$

where $T_b(x,y)$ and $T_I(x,y)$ ($I \in \{t, bt, tb, btb\}$) are defined in (1a-e).[8] Finally, substituting (4a-e) into (3) yields $\lambda_I(x,y)$.

Note that the transit-dominated route trip times depend on the numbers of boarding and alighting patrons (see Section 3.1), which in turn depend on the result of (5). Thus, the entire assignment process must be conducted via iteration (see the details in Section 4.2). In what follows, we develop some aggregate demand functions, including the transit boarding and alighting patron numbers (see equations (8-9) below). These functions will also be used in the cost models and constraints presented in the following sections.

First, the origin and destination density functions at location $u \in [0, L]$ for able-bodied patrons on route $I \in \{t, b, bt, tb, btb\}$, $b_I(u)$ and $a_I(u)$, are given by:

$$b_I(u) = \textstyle\int_{y=u}^{L} \lambda_I(u,y)dy\,,\, a_I(u) = \int_{x=0}^{u} \lambda_I(x,u)dx\,, I \in \{t, b, bt, tb, btb\}, u \in [0, L], \tag{6}$$

These can be deemed the approximate boarding and alighting densities for transit and bike modes[9] on respective routes. For example, $b_{bt}(u)$ represents the bike boarding density of patrons on route bt and $a_{bt}(u)$ the transit alighting density on the same route.

Similarly, the origin and destination densities for non-able-bodied patrons (who can only take route t), $\tilde{b}_t(u)$ and $\tilde{a}_t(u)$, are:

$$\tilde{b}_t(u) = \textstyle\int_{y=u}^{L} (1-\beta)\lambda(u,y)\, dy\,,\, \tilde{a}_t(u) = \int_{x=0}^{u} (1-\beta)\lambda(x,u)\, dx\,, u \in [0, L]. \tag{7}$$

Consequently, the total transit boarding and alighting densities at any location $x \in [0, L]$, $B_t(x)$ and $A_t(x)$, and the total bike picking-up and dropping-off densities, $B_b(x)$ and $A_b(x)$, are given by:

$$B_t(x) = \tilde{b}_t(x) + b_t(x) + b_{tb}(x) + \lambda_{b\to t}(x), \tag{8}$$

[8] Equation (5) can also be replaced by a stochastic route choice model, e.g., a logit model, to reflect the uncertainty in travelers' preference and perception.

[9] For simplicity, we still use terms "boarding" and "alighting" for shared bikes.

$$A_t(x) = \tilde{a}_t(x) + a_t(x) + a_{bt}(x) + \lambda_{t\to b}(x), \quad (9)$$

$$B_b(x) = b_b(x) + b_{bt}(x) + b_{btb}(x) + \lambda_{t\to b}(x), \quad (10)$$

$$A_b(x) = a_b(x) + a_{tb}(x) + a_{btb}(x) + \lambda_{b\to t}(x), \quad (11)$$

where $\lambda_{b\to t}(x)$ and $\lambda_{t\to b}(x)$ are the transfer demand densities from bike to transit and from transit to bike, respectively. They are approximated by $\lambda_{t\to b}(x) = a_{tb}(x) + a_{btb}(x)$ (note that routes tb and btb involve transfers from transit to bike that occur near the trip destinations) and $\lambda_{b\to t}(x) = b_{bt}(x) + b_{btb}(x)$.

Finally, the cross-sectional flows of bike and transit riders, $o_b(x)$ and $o_t(x)$ (patrons/h) at location $x \in [0, L]$, respectively, can be obtained by:

$$o_b(x) = \int_{u=0}^{x} (B_b(u) - A_b(u))du, \quad (12)$$

$$o_t(x) = o(x) - o_b(x), \quad (13)$$

where $o(x) = \int_{u=0}^{x}\int_{y=x}^{L} \lambda(u,y)dydu$ is the overall cross-sectional patron flow at $x \in [0, L]$.

3.3. Patrons' costs

Patrons' costs can be classified into four categories: (i) the total time for accessing and egressing transit stops and bike stations, $C_{a,t}$ and $C_{a,b}$; (ii) the total wait time at transit stops, $C_{w,t}$, and the total pick-up and drop-off lost times at bike stations, $C_{w,b}$; (iii) the total riding times in transit vehicles and on bikes, $C_{v,t}$ and $C_{v,b}$, respectively (the latter only accounts for the riding time on route b since the bike riding times for accessing/egressing transit stops were included in $C_{a,t}$); and (iv) the total transfer penalty, C_f. Formulations of these cost items are given in (14a-17):

$$C_{a,t} = \int_{x=0}^{L}\left(\frac{d_{ck}(x)(b_t(x)+b_{tb}(x)+a_t(x)+a_{bt}(x))}{2v_w} + \frac{\tilde{b}_t(x)+\tilde{a}_t(x)}{4\delta_t(x)v_w} + \frac{1}{2v_b}\left(\frac{1}{2\delta_t(x)} + d_{ck}(x)\right)\left(b_{bt}(x) + b_{btb}(x) + \lambda_{t\to b}(x)\right)\right)dx, \quad (14a)$$

$$C_{a,b} = \int_{x=0}^{L} \frac{b_{bt}(x)+a_{tb}(x)+\sum_{I\in\{b,btb\}}(b_I(x)+a_I(x))}{4\delta_b(x)v_w}dx, \quad (14b)$$

$$C_{w,t} = \int_{x=0}^{L} B_t(x)\frac{h}{2}dx, \quad (15a)$$

$$C_{w,b} = \int_{x=0}^{L}\left(t_{pu}B_b(x) + t_{do}A_b(x)\right)dx, \quad (15b)$$

$$C_{v,t} = \int_{x=0}^{L} \frac{o_t(x)}{V_t(x)}dx, \quad (16a)$$

$$C_{v,b} = \int_{x=0}^{L} \frac{\int_{u=0}^{x}(b_b(u)-a_b(u))du}{v_b}dx, \quad (16b)$$

$$C_f = \xi_{t\to b}\int_{x=0}^{L}\lambda_{t\to b}(x)dx + \xi_{b\to t}\int_{x=0}^{L}\lambda_{b\to t}(x)dx. \quad (17)$$

In (14a), the first term in the integrand is the average walking time to and from the closest transit stop for able-bodied patrons residing in the work-access/egress zones; see Figure 2. The second term is the average walking time for non-able-bodied patrons. The third term is the average bike-riding time to and from the closest transit stop. In (14b), the numerator of the integrand is the total bike demand density,

and $\frac{1}{4\delta_b(x)v_w}$ is the average access or egress time to or from the closest bike station by walking. Equation (15a) is self-evident by noting that $B_t(x)$ is the total transit boarding density and $\frac{h}{2}$ is the average wait time per patron. So is (15b) given the definitions of $B_b(x)$ and $A_b(x)$. Equations (16a) and (16b) are also easy to understand since the numerators in the integrands are cross-sectional flows of transit and bike riders (the latter only includes b-type trips), and the denominators are commercial speeds. Equation (17) is also self-explanatory.

Therefore, the total patron cost in transit and bike-sharing systems, C^U, is given by

$$C^U = C_{a,t} + C_{a,b} + C_{w,t} + C_{w,b} + C_{v,t} + C_{v,b} + C_f. \quad (18)$$

3.4. Agency costs

3.4.1. Transit agency costs

The transit service operator bears three types of costs: (i) infrastructure cost (e.g., capital and maintenance costs), denoted by $C_{l,t}$; (ii) distance-based operation cost (e.g., fuel cost), $C_{k,t}$; and (iii) time-based operation cost, $C_{h,t}$. They are estimated by (19-21), respectively.

$$C_{l,t} = \pi_l^t L + \pi_s^t \int_0^L \delta_t(x)dx, \quad (19)$$

$$C_{k,t} = \frac{\pi_k^t L}{h}, \quad (20)$$

$$C_{h,t} = \frac{\pi_h^t}{h} \int_0^L \frac{1}{V_t(x)} dx, \quad (21)$$

where π_l^t (\$/km/h) and π_s^t (\$/stop/h) in (19) are the amortized hourly costs per km of transit line and per stop, respectively; and π_k^t (\$/vehicle-km) and π_h^t (\$/vehicle-h) in (20, 21) are the unit distance-based and time-based operation costs, respectively.

Thus, the total agency cost of transit service, C_t^O, is obtained by

$$C_t^O = C_{l,t} + C_{k,t} + C_{h,t}. \quad (22)$$

3.4.2. Bike-sharing agency costs

The bike-sharing service operator bears the following cost components: (i) the infrastructure cost of bike stations, $C_{s,b}$; (ii) the purchase cost of bike fleet and docks, $C_{h,b}$; and (iii) the bike rebalancing cost for maintaining a spatial balance between the bike demand and supply, $C_{r,b}$. The first two are formulated as follows:

$$C_{s,b} = \pi_s^b \int_0^L \delta_b(x)dx, \quad (23)$$

$$C_{h,b} = \frac{(\pi_b^b + \varepsilon\pi_d^b)}{\rho} \int_0^L \left(\frac{o_b(x)}{v_b} + t_{pu} B_b(x) + t_{do} A_b(x) \right) dx, \quad (24)$$

where π_s^b (\$/station/h) denotes the amortized hourly cost of a bike station; π_b^b (\$/bike) and π_d^b (\$/dock) the unit costs of purchasing a bike and installing a dock, respectively; ε the ratio between the numbers of bikes and docks, which takes a value between 1.5 and 1.7 for real-world bike-sharing solutions (Tang

et al., 2011; Gleason and Miskimins, 2012; Gauthier et al., 2013; Yang et al., 2016; Wu et al., 2020); $\rho \in (0,1]$ the utilization ratio of shared bikes, i.e., the average proportion of time when a bike is in use; and the integrand in (24) yields the total bike-hours occupied for riding, pick-ups, and drop-offs. This type of formulations was also adopted by previous bike-sharing system planning studies (e.g., Lin and Yang, 2011). Precise determination of bike-sharing fleet can be done in the tactical design stage considering the spatio-temporal dynamics of bike flows among bike stations (Shu et al., 2013).

To estimate $C_{r,b}$, we assume that: (i) the rebalancing cost is proportional to the total bike-kms transported for the rebalancing purpose; and (ii) the rebalancing operation is performed once per hour. Following the idea in Nair and Miller-Hooks (2011), we propose a linear programming model to estimate $C_{r,b}$. The details are relegated to Appendix C.

Therefore, the total agency cost of bike-sharing service, C_b^O, is given by

$$C_b^O = C_{s,b} + C_{h,b} + C_{r,b}. \tag{25}$$

3.5. Optimization problem

We now formulate the joint optimal design problem that minimizes the overall generalized cost of the hybrid system as follows. The problem has two decision functions, $\delta_t(x)$ and $\delta_b(x), x \in [0, L]$, and one scalar decision variable, h.

$$\underset{\delta_t(x),\delta_b(x),h,x\in[0,L]}{\text{minimize}} \; Z = \sum_{i\in\{E,W\}} \left(C_i^U + \frac{1}{\mu}\left(C_{t,i}^O + C_{b,i}^O\right)\right) \tag{26a}$$

subject to:

$$h \geq h^{\min}, \tag{26b}$$

$$hO_t \leq K_t, \tag{26c}$$

$$\delta_b(x) \geq \delta_t(x), \quad x \in [0, L], \tag{26d}$$

$$\delta_t(x), \delta_b(x) \geq 0, \quad x \in [0, L], \tag{26e}$$

where Z is the total generalized cost measured by time. Note that both eastbound and westbound travel directions are considered in (26). This is done by appending a subscript $i \in \{E, W\}$ to all the direction-related variables in previous sections (e.g., cost components, boarding and lighting densities, and cross-sectional flows) to indicate the travel direction. The C_i^U, $C_{t,i}^O$, and $C_{b,i}^O$ are obtained from (18, 22, 25), respectively, for each direction $i \in \{E, W\}$. Constraint (26b) specifies that the headway must be no less than a minimum threshold, $h^{\min}$, to account for safety or road infrastructure capacity constraints. Constraint (26c) ensures that the transit system capacity is sufficient for carrying the patrons, meaning that no patron waiting at a stop will be left behind a vehicle. Here O_t is the maximum cross-sectional transit patron flow, and K_t is the vehicle capacity. The O_t can be estimated by $O_t = \max_{x\in[0,L],i\in\{E,W\}} \left(o_{t,i}(x)\right)$, where $o_{t,i}(x)$ is obtained from (13) for each direction $i \in \{E, W\}$. Constraint

(26d) guarantees that the bike station density is no less than the transit stop density anywhere in the corridor. The last constraint specifies the boundaries of the decision functions.

4. Solution Method

Section 4.1 presents the analytical results derived from the first-order conditions of (26). Built upon these results, Section 4.2 describes a bi-level heuristic algorithm for solving (26).

4.1. Analytical results

For now, we assume the route assignment (see Section 3.2) is fixed. Under this condition, program (26) can be decomposed into subproblems, each containing a few scalar variables, h, $\delta_t(x)$, and $\delta_b(x)$ for a specific $x \in [0, L]$. We further show in Appendix D that (26a) is a convex function of h, $\delta_t(x)$, and $\delta_b(x)$ (for a specific x) when only one variable is considered and all others are fixed. Further note that constraints (26b-e) are all boundary constraints. Thus, the optimal solutions $h^*, \delta_t^*(x)$, and $\delta_b^*(x)$ must satisfy the following equations derived from the first-order conditions of (26):

$$h^* = \text{mid}\left(h^{\min}, \tilde{h}, \frac{K_t}{O_t}\right), \tag{27}$$

$$\delta_t^*(x) = \sqrt{\frac{\sum_{i\in\{E,W\}}\left(\frac{\tilde{b}_{t,i}(x)+\tilde{a}_{t,i}(x)}{4v_w}+\frac{b_{bt,i}(x)+b_{btb,i}(x)+\lambda_{t\to b,i}(x)}{4v_b}\right)}{\left(\sum_{i\in\{E,W\}} o_{t,i}(x)+\frac{2\pi_h^t}{\mu h^*}\right)\tau^o+\frac{\pi_s^t}{\mu}}}, x \in [0, L], \tag{28}$$

$$\delta_b^*(x) = \max\left(\tilde{\delta}_b(x), \delta_t^*(x)\right), x \in [0, L], \tag{29}$$

$$\tilde{h} = \sqrt{\frac{2\pi_k^t L+2\pi_h^t\left(\frac{L}{v_t}+\int_{x=0}^{L}\tau^o\delta_t^*(x)dx\right)}{\mu\sum_{i\in\{E,W\}}\left(\int_{x=0}^{L}\frac{B_{t,i}(x)}{2}dx+\int_{x=0}^{L} o_{t,i}(x)\max\left(\tau^b B_{t,i}(x),\tau^a A_{t,i}(x)\right)dx\right)}}, \tag{30}$$

$$\tilde{\delta}_b(x) = \sqrt{\frac{\mu\sum_{i\in\{E,W\}}\left(b_{bt,i}(x)+a_{tb,i}(x)+\sum_{I\in\{b,btb\}}\left(b_{I,i}(x)+a_{I,i}(x)\right)\right)}{4v_w\pi_s^b}}, x \in [0, L], \tag{31}$$

where function $\text{mid}(\cdot)$ returns the middle value of the three arguments. Equations (28), (30) and (31) are derived by setting $\frac{\partial Z}{\partial \delta_t(x)} = 0$, $\frac{\partial Z}{\partial h} = 0$, and $\frac{\partial Z}{\partial \delta_b(x)} = 0$, respectively.

The above analytical results can help construct an iterative heuristic algorithm for solving (26), which is presented in the next section. They also unveil useful insights into the causal relationship between the optimal design and key operating factors. For instance, (28) reveals that the optimal transit stop density is positively correlated with the boarding and alighting densities of transit (see the numerator of the RHS), and negatively correlated with the cross-sectional transit patron flow (see the denominator). Other studies on transit corridor design have reported similar findings like the above (e.g., Wirasinghe and Ghoneim, 1981; Mei et al., 2021). In addition, (31) indicates that the optimal bike station density is correlated with the boarding and alighting densities of shared bikes.

4.2. A bi-level solution algorithm

Exploiting the optimality conditions (27-31), we propose a bi-level algorithm to solve (26a-e). The upper level determines the optimal design in terms of $h^*, \delta_t^*(x), \delta_b^*(x)$ ($x \in [0, L]$) given the route assignment. The lower level updates the route assignment given the new design. The two levels are iterated until convergence. Iterative algorithms of this fashion have been commonly used to solve bi-level optimization problems (e.g., network designs) involving network traffic assignment. To our best knowledge, however, most of these algorithms (including ours) cannot guarantee global optimality.

Detailed steps of the algorithm are described as follows:

Initialization: Discretize the corridor space $[0, L]$ into $\mathcal{M}$ equal segments, and define $\boldsymbol{X}$ as the set of segment midpoints, i.e., $\boldsymbol{X} = \{0.5\Delta x, 1.5\Delta x, \dots, (\mathcal{M} - 0.5)\Delta x\}$, where $\Delta x = \frac{L}{\mathcal{M}}$. Without introducing a new notation, we still use $\lambda(x, y)$ ($x, y \in \boldsymbol{X}$) to represent the demand from the segment containing x to the segment containing y. Equally assign the able-bodied demand to each route type, i.e., $\lambda_I(x, y)^{(0)} = \frac{\beta\lambda(x,y)}{5}$, $\forall\, I \in \{b, t, bt, tb, btb\}, x, y \in \boldsymbol{X}$. Randomly generate initial values of $\delta_b^{(0)}(\boldsymbol{X}), \delta_t^{(0)}(\boldsymbol{X}) > 0$ as well as $h^{(0)}$ satisfying constraints (26b-e). Set the number of iteration $n = 1$.

Upper level: *Determining the optimal design*

Step U0: Let $\bar{\delta}_b^{(0)}(\boldsymbol{X}) = \delta_b^{(n-1)}(\boldsymbol{X})$ and $\bar{\delta}_t^{(0)}(\boldsymbol{X}) = \delta_t^{(n-1)}(\boldsymbol{X})$. Set the upper-level iteration number $\overline{n} = 1$.

Step U1: Calculate headway $\bar{h}^{(\overline{n})}$ by (27) and (30) using $\bar{\delta}_t^{(\overline{n}-1)}(\boldsymbol{X})$ and $\bar{\delta}_b^{(\overline{n}-1)}(\boldsymbol{X})$. (Integrals in the equation are approximated by summations of the integrand function values at each point in $\boldsymbol{X}$.)

Step U2: Calculate stop densities $\bar{\delta}_t^{(\overline{n})}(\boldsymbol{X})$ by (28) using $\bar{h}^{(\overline{n})}$.

Step U3: Calculate the $\bar{\delta}_b^{(\overline{n})}(\boldsymbol{X})$ by (29) and (31). If $\overline{n} \geq N$ or the following convergence criterion (32) is satisfied, let $h^{(n)} = \bar{h}^{(\overline{n})}, \delta_t^{(n)}(\boldsymbol{X}) = \bar{\delta}_t^{(\overline{n})}(\boldsymbol{X})$, and $\delta_b^{(n)}(\boldsymbol{X}) = \bar{\delta}_b^{(\overline{n})}(\boldsymbol{X})$, and then go to the lower level. Otherwise, let $\overline{n} = \overline{n} + 1$ and go to Step U1.

$$\left|\frac{\bar{h}^{(\overline{n})} - \bar{h}^{(\overline{n}-1)}}{\bar{h}^{(\overline{n}-1)}}\right| + \sum_{x \in \boldsymbol{X}} \left|\frac{\bar{\delta}_t^{(\overline{n})}(x) - \bar{\delta}_t^{(\overline{n}-1)}(x)}{\bar{\delta}_t^{(\overline{n}-1)}(x)}\right| + \sum_{x \in \boldsymbol{X}} \left|\frac{\bar{\delta}_b^{(\overline{n})}(x) - \bar{\delta}_b^{(\overline{n}-1)}(x)}{\bar{\delta}_b^{(\overline{n}-1)}(x)}\right| \leq \alpha, \tag{32}$$

where α and N are predefined numbers. In this paper, we use $\alpha = 10^{-3}$ and $N = 10^3$.

Lower level: *Route assignment*

Step L0: Let $\bar{\lambda}_I(x, y)^{(0)} = \lambda_I(x, y)^{(n-1)}$ and set the lower-level iteration number $\overline{\overline{n}} = 1$.

Step L1: Reassign route demand as $\hat{\lambda}_I(x, y)$ using (3-5).

Step L2: Update the route demand by applying the method of successive averages (MSA) (Sheffi, 1985), i.e., $\bar{\lambda}_I(x, y)^{(\overline{\overline{n}})} = \bar{\lambda}_I(x, y)^{(\overline{\overline{n}}-1)} + \frac{\hat{\lambda}_I(x,y) - \bar{\lambda}_I(x,y)^{(\overline{\overline{n}}-1)}}{\overline{\overline{n}}}$.

Step L3: Let $\lambda_I(x, y)^{(n)} = \bar{\lambda}_I(x, y)^{(\overline{\overline{n}})}$ if (33) is satisfied or $\overline{\overline{n}} \geq N$, compute the aggregate demand functions using (6-13) and go to the Convergence-check step. Otherwise, set $\overline{\overline{n}} = \overline{\overline{n}} + 1$ and go to Step L1.

$$\max_{x,y\in \boldsymbol{X}} \left|\frac{\lambda_I(x,y)^{(\bar{n})}-\lambda_I(x,y)^{(\bar{n}-1)}}{\lambda_I(x,y)^{(\bar{n}-1)}}\right| \le \alpha. \quad (33)$$

Convergence check: Record the optimal solutions $h^* = h^{(n)}$, $\delta_t^*(\boldsymbol{X}) = \delta_t^{(n)}(\boldsymbol{X})$, $\delta_b^*(\boldsymbol{X}) = \delta_b^{(n)}(\boldsymbol{X})$ if (34) is satisfied or $n \ge N$. Otherwise, set $n = n + 1$ and return to the upper level.

$$\left|\frac{h^{(n)}-h^{(n-1)}}{h^{(n-1)}}\right| + \sum_{x\in \boldsymbol{X}} \left|\frac{\delta_t^{(n)}(\boldsymbol{X})-\delta_t^{(n-1)}(\boldsymbol{X})}{\delta_t^{(n-1)}(\boldsymbol{X})}\right| + \sum_{x\in \boldsymbol{X}} \left|\frac{\delta_b^{(n)}(\boldsymbol{X})-\delta_b^{(n-1)}(\boldsymbol{X})}{\delta_b^{(n-1)}(\boldsymbol{X})}\right| \le \alpha. \quad (34)$$

Solutions developed from the above algorithm cannot be directly applied to determine transit stop and bike station locations. We present a recipe to generate these exact locations in Appendix E.1.

5. Numerical studies

The set-up of numerical experiments is presented in Section 5.1. Section 5.2 examines the optimal hybrid system design and the accuracy of our CA model. Section 5.3 compares the performance of the hybrid design and the transit system design without shared bikes. Section 5.4 illustrates an application of our model for redesigning a real-world bus line in Chengdu, China.

5.1. Experiment set-up

Consider a hypothetical corridor with a length of $L = 20$ km. For the demand function, we use a modified version of the spatially heterogeneous demand function proposed by Vaughan and Cousins (1977). It takes the following form:

$$\lambda(x,y|\Lambda,\sigma_x^2,\sigma_y^2) = \Lambda\cdot\left(Tr\mathcal{N}(x|0,\sigma_x^2,0,L)Tr\mathcal{N}(y|L,\sigma_y^2,0,L) + Tr\mathcal{N}(x|L,\sigma_x^2,0,L)Tr\mathcal{N}(y|0,\sigma_y^2,0,L)\right), \quad (35)$$

where Λ (trips/h) denotes the total transit demand in each travel direction; $Tr\mathcal{N}(\cdot)$ denotes the PDF of a truncated normal distribution with the four parameters being in turn the mean, variance, left and right bounds of the support; σ_x^2 and σ_y^2 are parameters indicating how varied the spatial distributions of trip origins and destinations are. We can interpret this demand function as the product of the total demand in the corridor (2Λ) and the joint PDF of OD pair (x,y), i.e., $\frac{1}{2}\left(Tr\mathcal{N}(x|0,\sigma_x^2,0,L)Tr\mathcal{N}(y|L,\sigma_y^2,0,L) + Tr\mathcal{N}(x|L,\sigma_x^2,0,L)Tr\mathcal{N}(y|0,\sigma_y^2,0,L)\right)$. We choose this demand function due to two reasons. First, the function has only two parameters, σ_x^2 and σ_y^2, and is symmetric between the two travel directions. Second, the marginal PDFs of trip origins ($\frac{1}{2}\left(Tr\mathcal{N}(x|0,\sigma_x^2,0,L) + Tr\mathcal{N}(x|L,\sigma_x^2,0,L)\right)$) and trip destinations ($\frac{1}{2}\left(Tr\mathcal{N}(y|L,\sigma_y^2,0,L) + Tr\mathcal{N}(y|0,\sigma_y^2,0,L)\right)$)[10] can be independently specified to cover a wide range of demand patterns. The parsimony and generality of this demand function allow us to derive general insights by looking into a large battery of numerical instances.

[10] These marginal PDFs can be obtained by integrating the joint PDF with respect to y or x.

In addition, parameters σ_x^2 and σ_y^2 can be viewed as proxies for demand heterogeneity. Note that a larger σ_x^2 or σ_y^2 indicates that the trip origins or destinations are more evenly distributed over the corridor (i.e., the PDF curve is flatter). Particularly, $\sigma_x = \sigma_y = \infty$ is the uniform demand case. For illustration, Figures 3a and b plot the origin and destination densities and the cross-sectional flows for $\sigma_x = \sigma_y = 10$ km and $\sigma_x = \sigma_y = 5$ km, respectively. Comparison of the two figures manifests clearly that the demand is more heterogeneous with smaller values of σ_x and σ_y. In this paper, we use $\sigma_x, \sigma_y \in \{\infty, 10, 5\}$ km, and $\frac{\Lambda}{L} \in \{100, 150, 200, 250, 300\}$ trips/km/h.

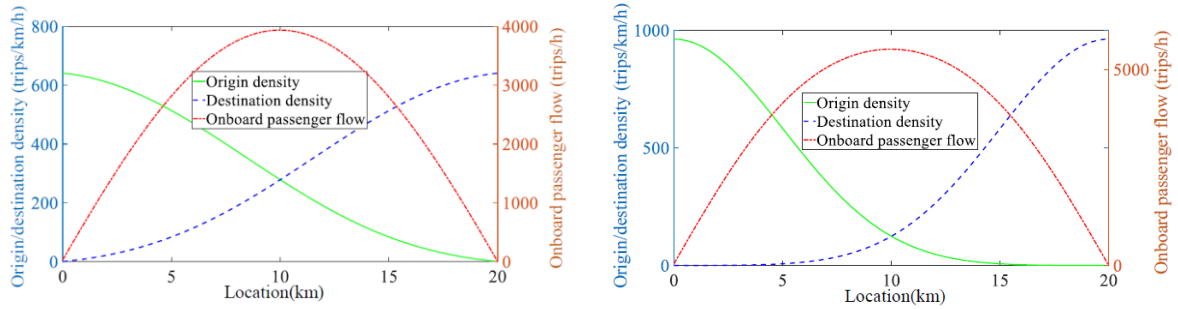

(a) Less-heterogeneous demand, $\sigma_x = \sigma_y = 10$ km

(b) More-heterogeneous demand, $\sigma_x = \sigma_y = 5$ km

Figure 3. Heterogeneous demand patterns ($\frac{\Lambda}{L} = 300$ trips/km/h).

In the following experiments, we consider two transit modes, i.e., bus and rail, and two alternative modes, i.e., shared bikes and electric scooters. By combination, we have four types of hybrid systems, i.e., bus-bike, rail-bike, bus-scooter, and rail-scooter. Parameter values regarding transit and alternative modes are summarized in Tables 1 and 2, respectively. They are all borrowed from previous studies (Daganzo, 2010; Sivakumaran et al., 2014; Chen et al., 2015; Gu et al., 2016; Bike to everything, 2019; Wu et al., 2020). Note that π_h^t, π_s^t, and π_l^t are assumed to be linear functions of the VOT μ to reflect the impacts of wage level on these cost rates. We specify that the average walking speed v_w is 2 km/h to account for the inconvenience of walking (Daganzo, 2010). The transit fare, φ_t, takes \$1/trip for bus and \$2/trip for rail. The $\{\varphi_k^1, \varphi_k^0\}$ are set to $\{5.59, 1.12\} \times 10^{-2}$\$ for bikes and $\{6.94, 2.31\} \times 10^{-2}$ \$ for scooters in a high-wage city, and $\{0.88, 0.18\} \times 10^{-2}$ \$ for bikes and $\{1.14, 0.38\} \times 10^{-2}$\$ for scooters in a low-wage city. These values were calculated using a model in Wu et al. (2020). Two VOTs, $\mu \in \{5, 25\}$ \$/h, are used to represent low- and high-wage cities, respectively. The discretization parameter $\mathcal{M}$ is set to 400, meaning that $\Delta x = 50$ m.

5.2. Optimal designs, accuracy of the CA model, and computation cost

We develop the optimal CA solutions of the hybrid system for 90 bus-corridor instances with $\frac{\Lambda}{L} \in \{100, 150, 200, 250, 300\}$ trips/km/h, $\sigma_x, \sigma_y \in \{\infty, 10, 5\}$ km, and $\mu \in \{5, 25\}$ \$/h. These instances reflect different combinations of demand levels and OD distributions in low- and high-wage cities.

Figure 4a illustrates the optimal bus stop spacing, $\frac{1}{\delta_t^*(x)}$, against $x \in [0, L]$ as the solid blue curve for the instance with $\sigma_x = \sigma_y = 5$ km, $\frac{\Lambda}{L} = 300$ trips/km/h, and $\mu = 5$ \$/h. The figure shows that the smallest stop spacings are observed at the corridor ends, while the largest occurs in the middle. This is because the total bus boarding and alighting density (the orange curve) reaches the highest at the corridor ends and the lowest in the middle. On the other hand, the cross-sectional patron flow exhibits the opposite trend (not shown). This verifies the finding revealed by (28); see Section 4.1.

Table 1. Parameter values for bus and rail systems.

Transit mode	v_t (km/h)	τ^0 (s)	τ^b, τ^a (s)	$h_t^{\min}$ (min)	K_t (patrons/veh)
Bus	25	30	2	1.5	80
Rail	60	45	0	2	2400
	π_k^t (\$/vehicle-km)	π_h^t (\$/vehicle-h)	π_s^t (\$/station/h)	π_i^t (\$/station/h)	$\xi_{t\to b}, \xi_{b\to t}$ (s)
Bus	0.59	2.66+3μ	0.42+0.014μ	6+0.2μ	30
Rail	2.2	101+5μ	294+9.8μ	594+19.8μ	90

Table 2. Parameter values for shared bike and electric scooter systems.

Mode	v_b (km/h)		ε		t_{pu}, t_{do} (s)		β	ρ
Bike	12		1.6		30		0.8	0.3
Scooter	20		1.6		30		0.8	0.3
	π_r^b (\$/bike-km)		π_s^b (\$/station/h)		π_b^b (\$/bike/h)		π_d^b (\$/dock/h)	
Cities / Mode	Low-wage	High-wage	Low-wage	High-wage	Low-wage	High-wage	Low-wage	High-wage
Bike	1	2	0.52	1.06	0.024	0.14	0.0044	0.036
Scooter	1	2	0.52	1.06	0.06	0.35	0.0044	0.036

Figure 4b plots the optimal bike station spacing, $\frac{1}{\delta_b^*(x)}$, also as the solid blue curve for the same instance. It shows that the bike station spacing follows a similar trend as the bus stop spacing, except that the former becomes slightly larger at the very ends of the corridor. The curve is again inversely correlated with the (bike) boarding and alighting density shown by the orange curve in Figure 4b. This correlation can be explained by (31). The increase of bike station spacings at the corridor ends is due to two reasons: (i) the access and egress mode share of biking is low at the corridor ends thanks to the small bus stop spacings; and (ii) the share of bike-only trips is also low at the corridor ends since patrons originating from or destined for corridor ends tend to prefer transit due to their longer trip distances. Finally, we see from Figure 4b that the optimal bike station spacings are small (in the range of 25-50m). This is mainly owing to the meager bike station installation cost.[11] Further analysis regarding the impacts of bike-sharing cost rates is presented in Section 5.3.4.

To examine the error brought by the continuum approximation technique, we also plot the exact bus stop and bike station spacings obtained using the recipe in Appendix E.1 as the dashed red curves in Figures 4a and b. Note how these curves closely match the solid blue curves.

[11] Such small spacings do exist in real practice. For example, the spacings between some dock-less shared-bike stations in Chengdu are below 20 m. Nevertheless, real-world bike station locations are subject to physical constraints, e.g., ramps and junctions. These constraints may affect the minimum bike station spacing in a city, but they are not considered in this paper.

Table 3 further summarizes the average percentage errors of various cost items between the CA solutions and the real design with exact bus stop and bike station locations for all 90 instances. Costs of the real design were calculated by the algorithm furnished in Appendix E.2. The table shows that the error in the generalized cost never exceeds 3%, and those in the itemized cost components never exceed 4%. This manifests the accuracy of our CA approach, which has been reported many times in the literature (e.g., Chen and Nie, 2017; Daganzo, 2010; Estrada et al., 2011).

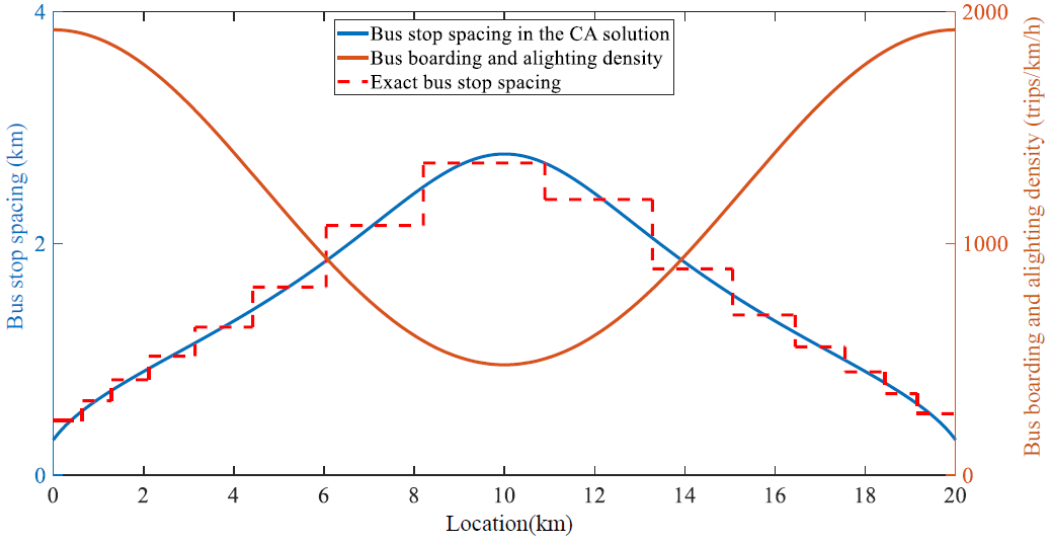

(a) Bus stop spacing

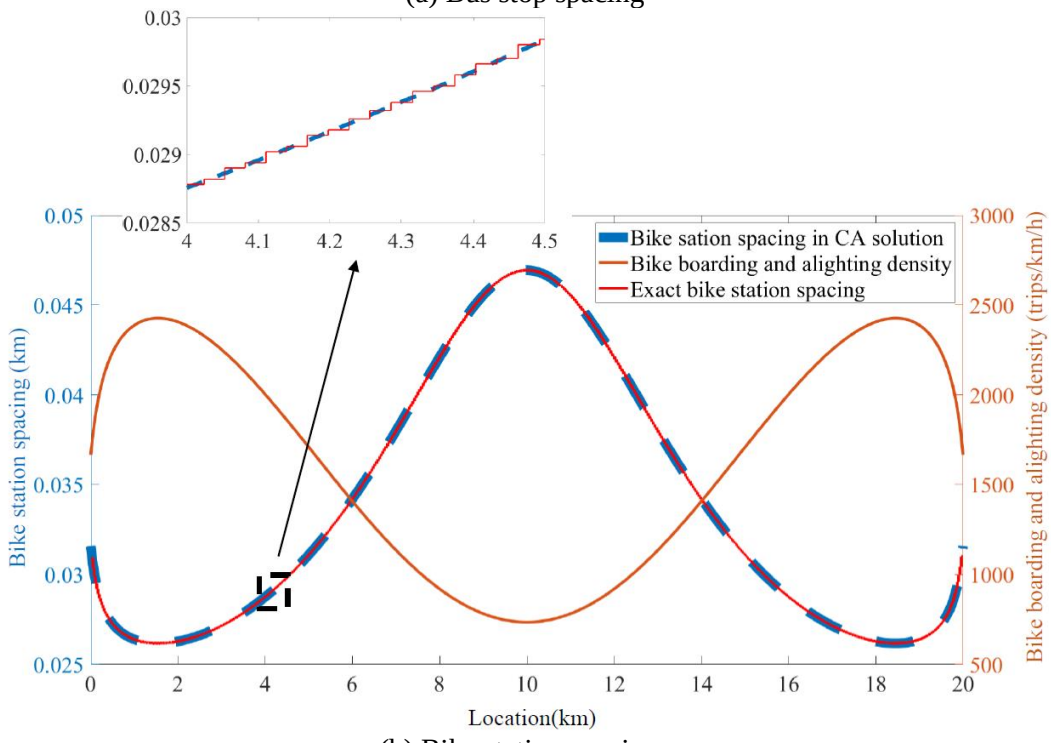

(b) Bike station spacings

Figure 4. CA and exact spacings of bus stops and bike stations.

We also examined the errors brought by the discretization method and the computational efficiency. We find that both the errors and the runtimes are within reasonable limits for a wide range of discretization parameter $\mathcal{M}$. Details are provided in Appendix F.

5.3. Parametric analysis

We next evaluate the percentage cost saving of the hybrid system compared to the transit system accessed by walking only, $\left(\frac{Z_s - Z_h}{Z_s}\right) \times 100\%$ (h/trip), where Z_h and Z_s are the generalized costs of the optimal hybrid and transit-only systems, respectively. Impacts on the cost saving from the following key operating factors are presented: demand level and variation (Section 5.3.1), alternative mode to shared bikes (Section 5.3.2), able-bodied patron ratio (Section 5.3.3), transit fare, bike rental fee, and bike-sharing agency cost rates (Section 5.3.4).

Table 3. Percentage cost errors of the CA solutions compared to the designs with exact bus stop and bike station locations.

	Average error (%)	Maximum error (%)
Generalized system cost	1.62	2.62
Patrons' cost	1.72	2.85
Access and egress time	1.13	1.48
Wait time and bike pick-up/drop-off time	2.26	3.94
In-vehicle travel time and bike riding time	0.58	0.67
Transfer time	1.83	3.3
Agencies' cost	0.63	1.62
Transit agency cost	0.65	1.95
Bike-sharing agency cost	0.60	0.72

5.3.1. Demand level and variation

In this section, we consider $\frac{\Lambda}{L} \in \{100,150,200,250,300\}$ trips/km/h and $\sigma_x = \sigma_y = \sigma \in \{\infty, 10,5\}$ km. Figures 5 and 6 show the performance of bus-bike and rail-bike systems under the five demand levels and three spatial variation levels in a high-wage city ($\mu = 25$ \$/h), respectively. Figure 5a shows that the cost saving of an optimal bus-bike system ranges in 12-16% and grows slowly as the demand level rises. Among the three spatial variation levels of demand, the highest percentage cost saving is achieved under the uniform demand case. This is partly because the uniform demand features a larger number of shorter trips that can be better served by bike only.

The economies of scale (EOS) for the two systems under all the three spatial variation levels are illustrated in Figure 5b. For each system and spatial variation level, we specify that the generalized cost under the demand $\frac{\Lambda}{L} = 100$ trips/km/h is 100%, and then plot the percentage change in cost per trip as the demand grows. The declining trend of each curve manifests that the optimal system exhibits EOS, i.e., that the cost per trip decreases as demand grows. Comparison between these curves shows that the uniform-demand case ($\sigma = \infty$) has the highest slope, meaning that its EOS is the strongest. On the other hand, the more heterogeneous demand case ($\sigma = 5$ km) exhibits the weakest EOS, possibly because the trip ends are more spatially concentrated near the corridor ends. Further comparison between the dashed

555 (bus-only systems) and solid (bus-bike systems) curves unveils that adding shared bikes would result in a stronger EOS. This echoes the finding that the hybrid system becomes more advantageous as demand grows. Similar results were also found for low-wage cities but are omitted here for brevity.

Results of rail-bike systems are also similar, as shown in Figures 6a and b. Comparison between Figures 5a and 6a shows that the rail-bike systems' cost savings are greater than bus-bike systems. This
560 is because shared bikes are better utilized in a rail-bike system due to the larger rail station spacings. Comparison between Figures 5b and 6b further reveals that the rail-bike systems exhibit stronger EOS, although adding shared bikes to a rail system has a lesser effect on the EOS.

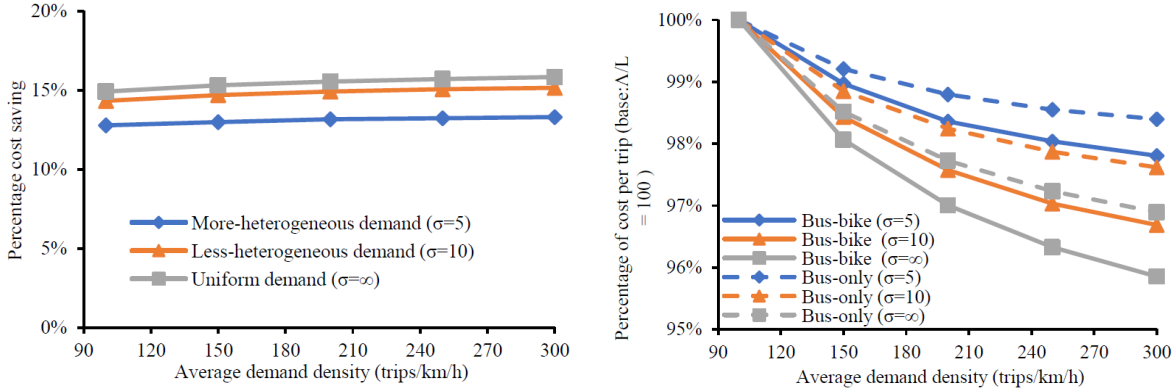

(a) Cost saving against a bus-only system (b) Percentage changes in the generalized cost

Figure 5. Performance of bus-bike systems.

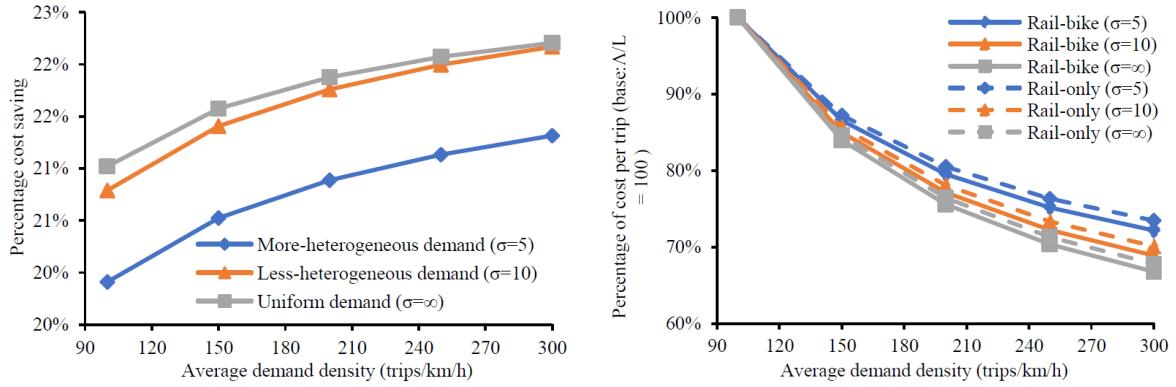

(a) Cost saving against a rail-only system (b) Percentage changes in the generalized cost

Figure 6. Performance of rail-bike systems.

565 In addition, closer observation unveils that cost reductions may be achieved for both the patrons and the operating agencies. Figures 7a and b show that this is true for bus-bike systems under the uniform demand and for rail-bike systems under all the demand patterns. The reason is simple: by incorporating shared bikes as a faster access mode, the optimal transit stop spacings become larger. The resulting transit agency cost savings can cover the expense of shared bikes. The agency cost savings
570 are greater for rail-bike systems because rail systems are more expensive. This finding is also consistent with a previous study (Wu et al., 2020).

5.3.2. Comparing shared electric scooters and shared bikes

Electric scooters are often used instead of bicycles as an access/egress mode and an alternative to transit. Table 4 presents the percentage cost savings of four hybrid systems (bus-bike, bus-scooter, rail-bike, and rail-scooter) compared to the transit-only systems in a high-wage city. The tabulated values show that all hybrid systems achieve cost savings. The transit-scooter systems appear to perform moderately better than the transit-bike systems.

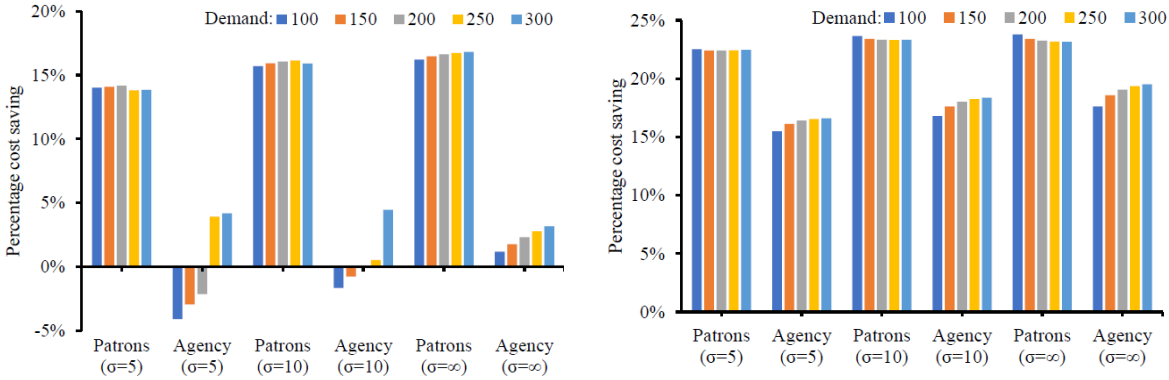

(a) Bus-bike systems (b) Rail-bike systems

Figure 7. Patron and agency cost savings.

Table 4. Impacts of different travel modes ($\frac{\Lambda}{L} = 300$ trips/km/h, $\mu = 25$ \$/h).

Hybrid systems	Demand patterns	Percentage cost saving	Share of able-bodied patron trips using bikes/scooters	
			bike/scooter-only trips	access/egress trips
Bus-bike	More-heterogeneous demand (σ=5)	13.30%	1.81%	76.75%
	Less-heterogeneous demand (σ=10)	15.14%	15.62%	63.16%
	Uniform demand (σ=∞)	15.83%	27.87%	50.97%
Bus-scooter	More-heterogeneous demand (σ=5)	21.33%	78.26%	1.30%
	Less-heterogeneous demand (σ=10)	23.07%	78.30%	1.29%
	Uniform demand (σ=∞)	25.50%	78.13%	1.39%
Rail-bike	More-heterogeneous demand (σ=5)	21.32%	1.92%	76.52%
	Less-heterogeneous demand (σ=10)	22.17%	14.7%	64.06%
	Uniform demand (σ=∞)	22.21%	25.26%	53.55%
Rail-scooter	More-heterogeneous demand (σ=5)	21.29%	7.26%	71.42%
	Less-heterogeneous demand (σ=10)	22.56%	33.51%	45.57%
	Uniform demand (σ=∞)	23.07%	48.68%	30.56%

Interestingly, the roles played by scooters and bikes in the hybrid systems are very different. This can be seen from columns 4 and 5 of Table 4. Column 4 shows the share of bike/scooter-only trips

(i.e., type b trips), and column 5 shows the share of transit trips accessed/egressed via bikes/scooters (i.e., type bt, tb, and btb trips), both among the trips made by able-bodied patrons. Specifically, shared bikes serve mainly as an access/egress mode to buses, while electric scooters are mostly used as an alternative to buses. This is due to the relatively high speed of scooters. For rail, however, both bikes and scooters mainly function as access/egress modes, owing to the high speed of rail transit and the large rail station spacings. The above findings confirm the observations in empirical studies (Ma et al., 2015; Graehler Jr. et al., 2019). The tabulated values also unveil that as the demand becomes more heterogeneous (i.e., as σ increases), the share of direct trips served by bikes/scooters generally decreases while the share of access/egress trips increases. This finding is also as expected since a larger σ renders more long trips that are better served by transit.

5.3.3. Able-bodied patron ratio

The able-bodied patron ratio varies across cities with different terrains, climates, and bike-friendly infrastructures. Figure 8 shows how the percentage cost saving of a bus-bike system increases with this ratio for $\frac{\Lambda}{L} = 300$ trips/km/h in a high-wage city. The curves show that benefits (although small) are achieved even when this ratio is as low as 10%. This is expected since as the able-bodied patron ratio diminishes, the optimal hybrid design will feature a smaller-scale bike-sharing service with a lower bike station density (subject to constraint (26d)) and fewer bikes and docks. In the extreme case where no patron uses bikes, the numbers of bikes and docks will reduce to zero, and the optimal design will be similar to a transit-only one. Similar results were observed for other hybrid systems involving rail transit or scooters.

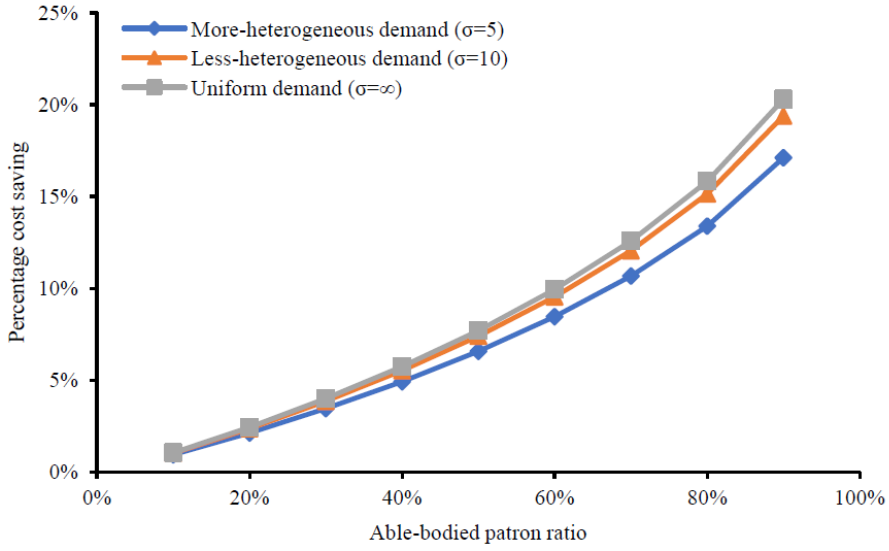

Figure 8. Cost savings of bus-bike systems versus the able-bodied patron ratio.

5.3.4. Transit fare, bike rental fee, and bike-sharing agency cost rates

Figure 9a plots the bus-bike system's percentage cost saving against $\varphi_t \in [0,2]$ \$/trip for $\frac{\Lambda}{L} = 300$ trips/km/h in a high-wage city. Curves in the figure show that the cost saving diminishes as bus fare increases since more patrons will be forced to choose cycling instead of buses. The uniform demand case exhibits the highest sensitivity to the bus fare. This is because the uniform demand pattern features more short trips, and those short trips are more sensitive to a high bus fare.

Figure 9b illustrates the effect of bus fare on the optimal hybrid system design. For simplicity, the average bus stop spacing is plotted as a proxy of the optimal design against $\varphi_t \in [0,10]$ \$/trip for $\frac{\Lambda}{L} = 300$ trips/km/h in a high-wage city. The figure reveals that the optimal stop spacings decrease moderately as φ_t grows. This is because more able-bodied patrons are priced out of bus rides due to the high fare. The remaining bus patrons, consisting mainly of non-able-bodied patrons that must walk to access and egress bus stops, call for shorter stop spacings. The optimal bike station spacings exhibit a similar trend because the bike demand grows with φ_t. The details are however skipped in the interest of brevity. Similar findings were also observed for rail-bike systems.

The impacts of bike rental fee on the hybrid system's cost saving and optimal design are presented in Figures 10a-d, again for bus-bike systems in a high-wage city with $\frac{\Lambda}{L} = 300$ trips/km/h. Figures 10a and b show that the cost saving is rather insensitive to φ_k^0 and φ_k^1 (note the very small ranges of vertical axes of these figures). The change of cost saving is visible only for the uniform demand case in Figure 10b and only when φ_k^1 is small. Further analysis shows that the cost saving declines when $\varphi_k^0 > 1$ \$ or $\varphi_k^1 > 5$ \$/km, which is expected because higher bike rental fees will force most cyclists to choose walking or transit instead. Details of these results are omitted here because such fees are too high even for high-wage cities. Optimal bike station spacings are also insensitive to the bike fee rates, as shown in Figures 10c and d. The curves exhibit a modest increasing trend since growing bike fees will reduce the bike demand, rendering larger bike station spacings. Insensitivity to bike fee rates is also observed for transit stop spacings (again omitted for simplicity).

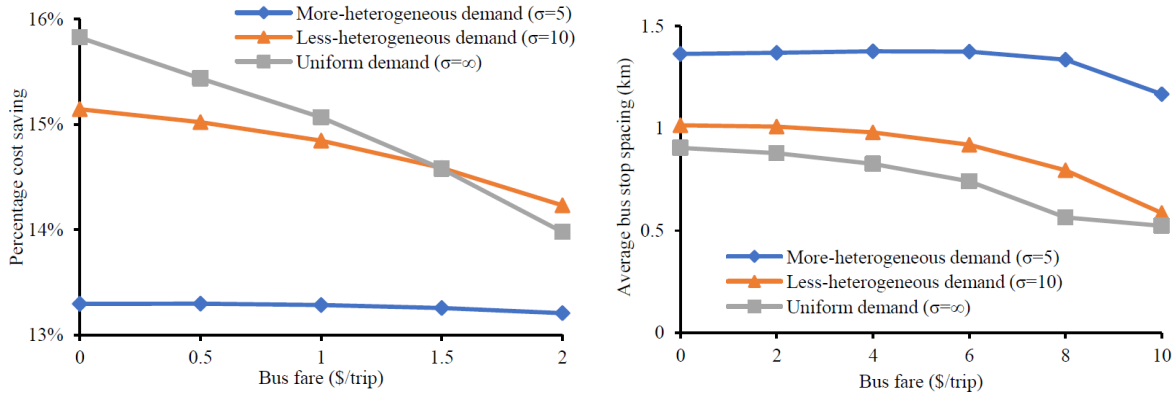

(a) Cost saving versus fare (b) Bus stop spacings versus fare

Figure 9. Impacts of fare on bus-bike systems.

We further examine the impacts of bike-sharing agency cost rates (i.e., π_r^b, π_s^b, π_b^b, and π_d^b) using the same numerical instances with $\frac{\Lambda}{L} = 300$ trips/km/h and $\mu = 25$ \$/h. The hybrid design's percentage cost saving and the average bike station spacing are plotted in Figures 11a and b against an amplifying factor of the above cost rates, which takes values from 1 to 5. For parsimony, we assume all those cost rates are multiplied by the same amplifying factor. As expected, the advantage of the hybrid design declines as those cost rates rise. Fortunately, however, the declination is slight; see in Figure 11a that the hybrid design still renders a cost saving of over 10% if shared bikes are five times as expensive as the cost rates we used before. On the other hand, Figure 11b shows that the optimal bike station spacings increase rapidly with the cost rates. Transit design is again insensitive to the bike-sharing agency cost rates, and the results are yet again omitted for brevity. Similar findings have also been observed for hybrid systems with other modes, different demand patterns, and VOTs.

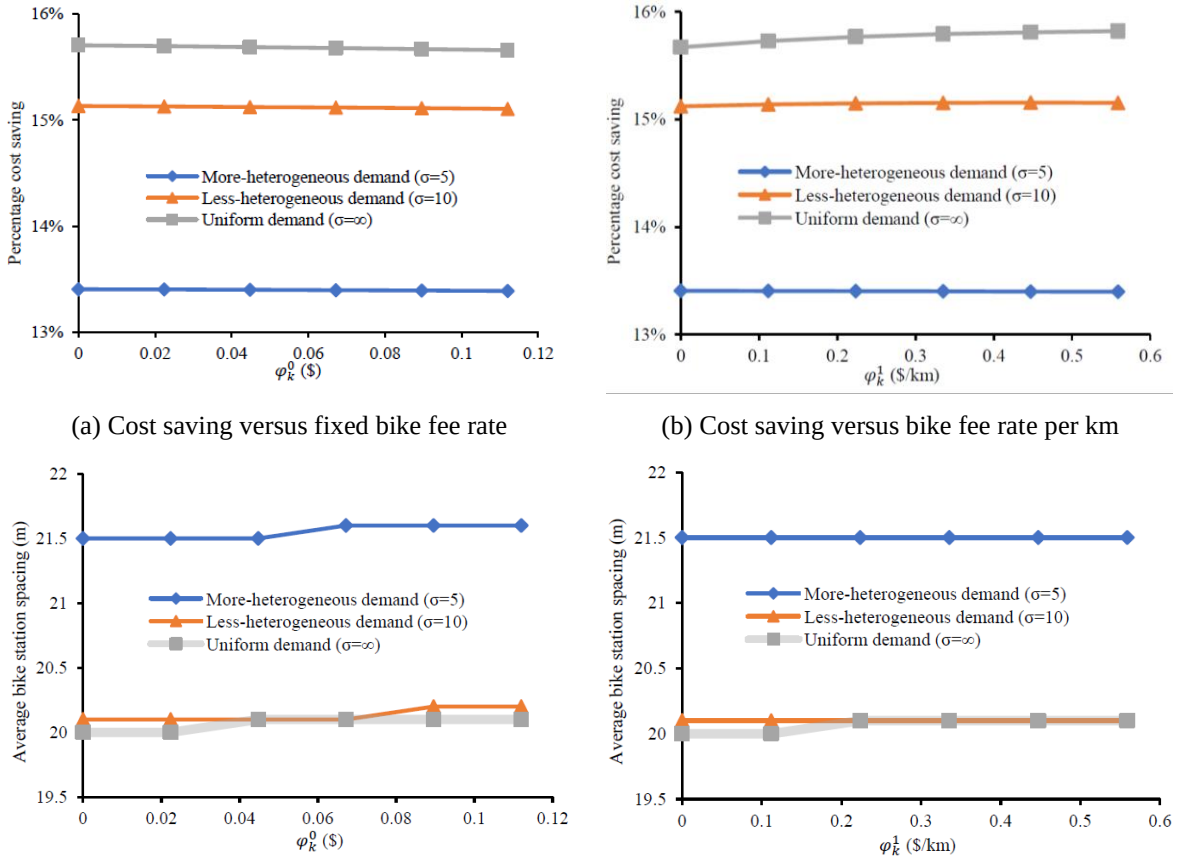

(a) Cost saving versus fixed bike fee rate

(b) Cost saving versus bike fee rate per km

(c) Bike station spacings versus fixed bike fee rate

(d) Bike station spacings versus bike fee rate per km

Figure 10. Impacts of bike rental fees on bus-bike systems.

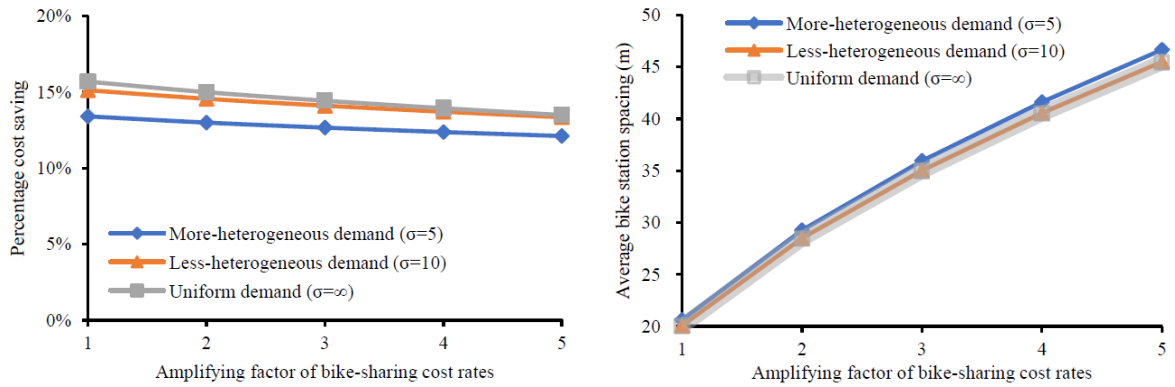

(a) Changes in cost saving (b) Changes in bike station spacings

Figure 11. Impacts of bike-sharing agency cost rates on bus-bike systems.

5.4. Real-world case study

Lastly, we illustrate how the proposed model is applied to reoptimize Bus Line No. 1 in Chengdu, China. The 14.23-km long bus line currently contains 27 stops. We collected the actual stop-to-stop OD data on May 10th, 2016, and approximated it by a continuous function using a surface-fitting tool, Gridfit in Matlab. Figure 12 illustrates the fitted continuous demand function. A low VOT, μ =5 \$/h, is used to represent the social wealth level in Chengdu. Other model parameters are the same as in Section 5.1. Note that no shared bike was available in Chengdu when the demand data was collected. Thus, we can reasonably assume that all bus patrons walk for access and egress in the "present-day scenario."

We compare the present-day scenario of the bus line and the following three alternatives: (i) where the bus stop locations and headway are optimized without considering shared bikes, termed the "Bus-only" scenario; (ii) where the bike-sharing system is jointly optimized with the bus line, termed the "Hybrid-design" scenario; and (iii) where the shared bikes are added to the current bus line with fixed stop locations, and only the bus headway and the bike station density are optimized, termed the "Adding-bikes" scenario. The last scenario is common when shared bikes are integrated with an existing rail line instead of a bus line.

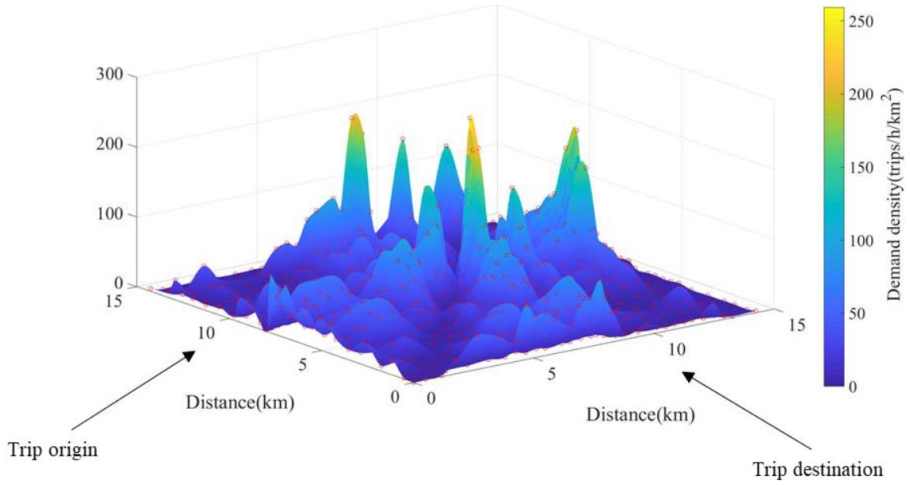

Figure 12. The approximate demand function for Bus Line No. 1 of Chengdu.

We first examine the optimal hybrid design. The optimal bus-stop and bike-station spacings from the CA solution are plotted as the dashed and solid curves in Figure 13. The exact bus stop locations are marked by the blue circles. The figure also plots the present bus stop spacing as the dotted curve and marks the stop locations as black squares for comparison. The curves show that the optimal bus stop spacings vary between 400 and 1200 m. They are significantly greater than the present ones in the middle part of the bus route, while they roughly match each other near the route ends. The optimal bike station spacings vary between 30 and 100 m.

Table 5 summarizes the key design variables and cost components for the present-day scenario and the three alternatives. Note first that the optimal headways in all the three alternatives are lower than the present one, indicating that the present service frequency is too low. Second, the hybrid design produces a greater average stop spacing than both the present-day and Bus-only alternatives. This confirms that optimally integrating a shared-bike system would significantly increase transit stop spacings. In addition, the optimal hybrid design features a lower average bike station spacing than the Adding-bikes alternative since fewer patrons choose cycling in the latter alternative due to the fixed (and smaller) bus stop spacings.

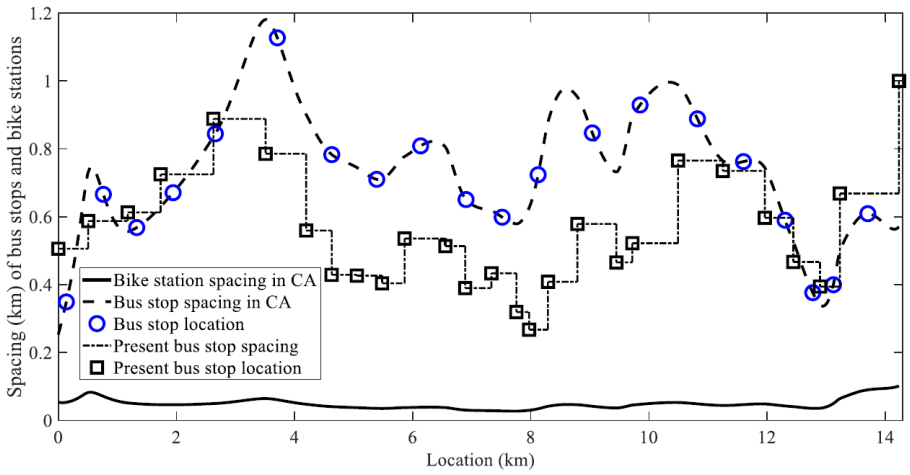

Figure 13. The optimal hybrid design of Bus Line No. 1.

All the three alternatives attain cost savings compared to the present-day scenario. The optimal hybrid design produces the greatest cost saving of 23.8%. Happily, even the Adding-bikes scenario, where bus stop locations were not reoptimized, can attain a cost saving of 20.11%, which is 9% higher than the Bus-only alternative. Cost breakdown further shows that the optimal hybrid design and the Adding-bikes alternative produce lower costs for both patrons and agencies than the Bus-only scenario. This result confirms that jointly operating shared bikes with transit may benefit the transit agency. Thus, the hybrid design holds much promise in reality.

Table 5. Comparison of different scenarios for the case study.

Metrics	Present-day	Bus-only	Hybrid-design	Adding-bikes
h_t (mins)	4	2.72	3.12	3.31
Average bus stop spacing (km)	0.53	0.39	0.83	0.53
Average bike station spacing (km)	/	/	0.05	0.07

Average generalized cost (mins/patron)	29.57	26.26	22.53	23.62
Generalized cost saving (%)	/	11.21	23.80	20.11
Average patron cost (mins/patron)	27.31	22.84	19.41	20.54
Average agency cost (mins/patron)	2.26	3.41	3.12	3.08

6. Conclusions

This paper proposes a CA model for optimally designing a hybrid mobility system consisting of shared-bike (or shared-electric-scooter) and transit services in corridors. The proposed model considers that shared bikes can be used as both a substitute (in the bike-only routes) and a complement (i.e., feeders) to transit. Built upon patrons' route choices, the model identifies the optimal transit service headway, transit stop spacings, and bike station spacings that minimize the total system cost. A bi-level solution algorithm was developed that exploits some analytical properties of the optimal solution derived from the parsimonious CA model. Numerical experiments verified the accuracies of the continuum approximations and the discretization method used in our solution approach. Practical use of our model was demonstrated via an application to a real bus line. To our best knowledge, this paper is the first that examines the joint optimization of shared-bike and transit services considering realistic route choices under spatially heterogeneous demand.

The analytical properties derived from our CA model reveal insights regarding the optimal hybrid design, which were overlooked by previous studies that assumed a uniform demand pattern. For example, the transit stop spacing is positively correlated with the transit boarding and alighting densities everywhere in the corridor. A similar finding is also reported for the bike station spacing.

Our numerical experiments also unveiled new insights that have practical implications. First, optimally integrating a shared-bike service within a transit corridor can significantly reduce the generalized cost for most instances investigated. Greater cost savings are observed for rail corridors, higher demand levels, and higher proportions of shorter trips (i.e., the uniform demand case in our analysis); see Section 5.3.1. The cost saving is generally insensitive to key operating parameters, including the transit fare, bike rental fee, and bike-sharing agency cost rates; see Section 5.3.4. Furthermore, cost savings are attained even when shared bikes are added to an existing transit (e.g., rail) line whose stops cannot be relocated; see Section 5.4. These findings manifest the sizeable potential benefit for incorporating shared micro-mobility solutions (e.g., shared bikes and electric scooters) with transit systems. Moreover, cost savings are incurred by both the patrons and the operating agencies under certain operating conditions; see again Figure 7. This implies that operating a bike-sharing system can be profitable for the transit agency.

On the other hand, the benefit of the hybrid design depends largely on the ratio of patrons who can and are willing to ride bicycles; see Section 5.3.3. This indicates the importance of bike-friendly facilities (e.g., bike lanes) and incentives (e.g., transit fare discounts for shared-bike riders) for the success of a hybrid system.

Lastly, we find that under various mode combinations and demand levels, both the shares of direct trips and feeder trips by bike (or scooter) can be significant; see Section 5.3.2. This confirms the necessity of modeling all the five route options in Section 3.2.

Our model can be built upon to explore more realistic features of hybrid systems. For example, the deterministic route choice model presented in Section 3.2 can be replaced by a stochastic one incorporating patrons' various preferences if the patron behavior data are available. Environmental impacts (e.g., greenhouse gas emission) can also be included in our objective function to examine how they would affect the optimal design (Sun, 2017). In addition, one may also consider the possibility that cyclists may take shortcuts while transit routes may have detours, and that the cyclists' biking cost per km would be higher on roads with slopes (Ceder et al., 2015). Our model can be modified to incorporate these realistic factors, for example, by using a location-dependent cycling speed to account for the different distances and times traveled by bike between any two points in a corridor. Finally, the present study can also be extended to model hybrid network designs in a city. The transit network structure can take the special forms proposed by earlier studies (e.g., Chen et al., 2018; Badia, 2020) or more general forms currently under development.

Acknowledgments

The research was supported by funds provided by the National Natural Science Foundation of China (No. 51608455), Sichuan Provincial Science & Technology Innovation Cooperation Funds (No. 2020YFH0038), and a General Research Fund (No. 15224818) provided by the Research Grants Council of Hong Kong. Helpful comments from two anonymous reviewers are greatly appreciated.

Appendix A: Notations

Table A1. Table of notations.

Notation	Descriptions	Units
Decision variables		
$\delta_t(x)$	Transit stop density at location x	stops/km
$\delta_b(x)$	Bike station density at location x	stations/km
h	Transit service headway	h
Other notations		
$a_{I,i}(x), \tilde{a}_{t,i}(x)$	Alighting densities of able-bodied patrons on route I, and of non-able-bodied patrons, at location x in direction i	trips/km/h
$A_{t,i}(x), A_{b,i}(x)$	Transit alighting density and bike drop-off density at location x in direction i	trips/km/h
$b_{I,i}(x), \tilde{b}_{t,i}(x)$	Boarding densities of able-bodied patrons on route I, and of non-able-bodied patrons, at location x in direction i	trips/km/h
$B_{t,i}(x), B_{b,i}(x)$	Transit boarding density and bike pick-up density at location x in direction i	trips/km/h
d_{ck}	Critical distance for determining the access/egress mode	km
$f(x)$	Average bike-as-feeder riding time for a patron at location x	h
$h^{\min}$	Minimum headway of transit service	h
K_t	Transit vehicle capacity	patrons/vehicle
O_t	Maximum cross-sectional flow in the transit line	patrons/h
$o_b(x), o_t(x)$	Cross-sectional flows of bike riders and transit patrons at location x	patrons/h
$\mathcal{P}_I(x,y)$	Choice probability of route I for a trip from x to y	
$T_I(x,y)$	Travel time of route I for a trip from x to y	h
t_{pu}, t_{do}	Pick-up and drop-off delays of a bike at a bike station	h
$V_t(x)$	Commercial transit speed at location x	km/h
v_t, v_b, v_w	Cruising speed of transit vehicle, cycling speed, and walking speed	km/h
Z	Total generalized system cost	h
$\lambda(x,y)$	Travel demand density from x to y	trips/km^2/h
$\lambda_I(x,y)$	Travel demand density of route I from x to y	trips/km^2/h
$\lambda_{b\to t}(x), \lambda_{t\to b}(x)$	Transfer demand densities from bike to transit and from transit to bike at location x	trips/km/h
β	Able-bodied patron ratio	
μ	Value of time	\$/h
τ^o, τ^b, τ^a	Fixed delay per transit stop, and delays per boarding and alighting patrons	h
ε	Ratio between the numbers of bikes and docks	
ρ	Utilization ratio of shared bikes	
$\varphi_t, \varphi_k(d)$	Flat transit fare and the distance-based bike rental fee	\$
$\xi_{b\to t}, \xi_{t\to b}$	Transfer penalties from bike to transit and from transit to bike.	h/transfer

Appendix B: Proof of Proposition 1 and derivation of $d_{ck}(x)$

Let MAC_{b-w} be the marginal cost of the hybrid system brought by a patron who switches from walking to cycling for accessing the nearest transit stop; it can be formulated as

$$MAC_{b-w} = \left(\frac{d}{v_b} + \frac{\varphi_k(d)}{\mu} + \kappa_b + t_{pu} + t_{do} + \xi_{b\to t}\right) - \frac{d}{v_w} \quad \text{(B1)}$$

where d denotes the access distance to the nearest transit stop; $\varphi_k(d)$ the bike rental fee as a *linear* function of d; μ the VOT (\$/h); κ_b the walking time to the nearest bike station, which can be approximated by $\frac{1}{4v_w\delta_b(x)}$ for location $x \in [0, L]$; v_b and v_w the bike and walking speeds; t_{pu}, t_{do}, and $\xi_{b\to t}$ the times lost to bike pick-up, drop-off, and transfer from a bike station to the neighboring transit stop, respectively.

Since MAC_{b-w} is a linear function of d, a unique critical distance $d_{ck}(x) = \min\left(d|MAC_{b-w}(d) = 0, \frac{1}{2\delta_t(x)}\right)$ can be found for any $x \in [0, L]$, such that:

i) if $d < d_{ck}(x)$, then $MAC_{b-w} > 0$, and the patron will choose walking.

ii) if $d > d_{ck}(x)$, then $MAC_{b-w} < 0$, and the patron will choose to ride a bike.

iii) if $d = d_{ck}(x)$, then $MAC_{b-w} = 0$, and the patron is indifferent between walking and cycling.

The same result applies to the egress mode choice, except that $\xi_{b\to t}$ in (B1) is replaced by the transfer penalty from transit to bike, $\xi_{t\to b}$.

Appendix C: Estimation of $C_{r,b}$

The rebalancing cost estimation problem is formulated as the following cost minimization problem:

$$C_{r,b} = \underset{g(x,y)}{\text{minimize}}\, \pi_r^b \int_0^L \int_0^L |x - y| g(x,y) dx dy \tag{C1a}$$

subject to:

$$N_b^+(x) = \int_{y=0}^{L} g(x,y)dy\,, x \in [0, L], \tag{C1b}$$

$$N_b^-(x) = \int_{y=0}^{L} g(y,x)dy\,, x \in [0, L], \tag{C1c}$$

$$g(x,y) \geq 0, \tag{C1d}$$

where $g(x,y)$ is the number of bikes redistributed from location x to y per hour; and π_r^b (\$/bike-km) the unit transport cost per bike-km. Constraints (C1b-c) guarantee the bikes are balanced at any location x, where $N_b^+(x)$ and $N_b^-(x)$ denote the local redundancy and shortage of bikes per hour of operations, respectively. They are given by:

$$N_b^+(x) = \max\left\{\sum_{i\in\{E,W\}}\left(A_{b,i}(x) - B_{b,i}(x)\right), 0\right\}; \tag{C2}$$

$$N_b^-(x) = \max\left\{\sum_{i\in\{E,W\}}\left(B_{b,i}(x) - A_{b,i}(x)\right), 0\right\}. \tag{C3}$$

To solve program (C1), we first discretize the corridor into $\mathcal{M}$ equal segments and define $\boldsymbol{X}$ as the set of $\mathcal{M}$ midpoints of these segments (see Section 4.2 for a similar treatment). We discretize the decision function $g(x,y)$ and all the continuous spatial functions in (C1-C3) into values taken on $\boldsymbol{X}$. Program (C1) then becomes a linear program with $\mathcal{M}^2$ decision variables $\{g(x,y), x, y \in \boldsymbol{X}\}$. We solve it using the "linprog" tool in MATLAB 2018a.

Appendix D: Proof of the convexity of (26a) concerning each decision variable individually

We first prove the convexity of (26a) concerning h only, assuming that $\delta_b(x)$ and $\delta_t(x)$ for all $x \in [0, L]$ are fixed. By reorganizing the terms involving h, the objective function (26a) can be rewritten as:

$$Z_h = \gamma_{h1} h + \gamma_{h2} h^{-1} + \gamma_{h3} \quad \text{(D1)}$$

where γ_{h1}, γ_{h2}, and γ_{h3} are unrelated to h, and $\gamma_{h1}, \gamma_{h2} > 0$. Thus, Z_h is a convex function of h. Note that the unconstrained optimal solution of h is $\tilde{h} = \gamma_{h2}^{1/2} \gamma_{h1}^{-1/2}$. This leads to (30).

Similarly, by fixing h and $\delta_b(x)$ ($\forall x \in [0, L]$), (26a) can be rewritten as:

$$Z_t = \int_{x=0}^{L} \left(\gamma_{t1}(x)\delta_t(x) + \gamma_{t2}(x)\delta_t^{-1}(x)\right)dx + \gamma_{t3} \quad \text{(D2)}$$

where for any $x \in [0, L]$, $\gamma_{t1}(x)$, $\gamma_{t2}(x)$, and γ_{t3} are unrelated to $\delta_t(x)$, and $\gamma_{t1}(x), \gamma_{t2}(x) > 0$. Thus, Z_t is a convex function of $\delta_t(x)$ for any $x \in [0, L]$. Here the unconstrained optimal solution of $\delta_t(x)$ is $\delta_t^*(x) = \gamma_{t2}^{\frac{1}{2}}(x)\gamma_{t1}^{-\frac{1}{2}}(x)$. This yields (28).

The convexity concerning $\delta_b(x)$ and (31) can be derived similarly.

Appendix E: Discretization recipe and cost models for real-world designs

E.1. A recipe to derive the exact transit stop and bike station locations from a CA solution

Step 1: Preparation. Fit the discrete optimal solutions, $\delta_b^*(\boldsymbol{X})$ and $\delta_t^*(\boldsymbol{X})$, to continuous functions $\delta_b^*(x)$ and $\delta_t^*(x)$ ($x \in [0, L]$) using, e.g., the spline curve fitting method.

Step 2: Locating transit stops. Place one transit stop at every location x where $\int_{u=0}^{x} \frac{du}{\delta_t^*(u)} - \frac{1}{2}$ yields an integer. Let $\boldsymbol{\Omega_t} = \{x_j^t | j = 1,2, \dots, n_t\}$ be the set of stop locations generated, where n_t is the total number of transit stops, and x_j^t the location of jth transit stop satisfying $0 < x_1^t < x_2^t < \cdots < x_{n_t}^t \leq L$.

Step 3: Locating bike stations. Find the set of bike station locations, $\boldsymbol{\Omega_b} = \{x_k^b | k = 1,2, \dots, n_b\}$, where n_b is the total number of bike stations, and x_k^b the location of kth bike station satisfying $0 < x_1^b < x_2^b < \cdots < x_{n_b}^b \leq L$ and $\int_{u=0}^{x_k^b} \frac{du}{\delta_b^*(u)} - \frac{1}{2}$ being an integer. Match the closest bike station to each transit stop.

E.2. Computing cost items for real-world designs with exact transit stop and bike station locations

The following algorithm computes cost items for the eastbound direction. Those for the westbound direction can be similarly computed.

Step 0. Preparation.

Define the catchment zone of the m-th bike station ($m = 1, \dots n_b$) as the continuous segment bounded on the left by $l_m^b = \frac{x_{m-1}^b + x_m^b}{2}$ and on the right by $r_m^b = l_{m+1}^b$ ($x_0^b = 0$ and $x_{n_b+1}^b = L$).

Similarly, define the catchment zone of the j-th transit stop ($j = 1, \dots, n_t$) as bounded by $l_j^t = \frac{x_{j-1}^t + x_j^t}{2}$ and $r_j^t = l_{j+1}^t$ ($x_0^t = 0$ and $x_{n_t+1}^t = L$). Here n_b and n_t are the numbers of bike stations and transit stops, respectively; and x_m^b and x_j^t are the locations of the k-th bike station and the j-th transit stop, respectively (see Appendix E.1). Determine the critical distance for each transit stop j, denoted d_{ck}^j, using the method proposed in Appendix B.

Step 1. OD matrix generation and route assignment.

Step 1.1. Generate the station-to-station OD matrix: $\lambda_{o,d} = \int_{l_o^b}^{r_o^b} \int_{l_d^b}^{r_d^b} \lambda(x,y) dy dx$, $1 \le o < d \le n_b$.

Step 1.2. For each OD pair (o, d), check if x_o^b or x_d^b is within the walk-access zone of the nearest transit stop, whose number is denoted j_o or j_d, by comparing the distance $d_m^{j_m} = \left| x_m^b - x_{j_m}^t \right|$ ($m \in \{o, d\}$) with the critical distance $d_{ck}^{j_m}$. Define indicator variables: $H_m^{j_m} = 1$ if $d_m^{j_m} \le d_{ck}^{j_m}$, and $H_m^{j_m} = 0$ otherwise for $m = 1,2, \dots, n_b$. Find the least-cost transit-dominated route among $\{t, bt, tb, btb\}$ for OD pair (o, d) by examining $H_o^{j_o}$ and $H_d^{j_d}$.

Step 1.3. Set an initial demand assignment between transit-dominated routes and the bike-only one. For each (o, d), compute the trip time involving transit, $T_{o,d}^t$, and the bike-only trip time, $T_{o,d}^b$. Reassign the able-bodied demand of each OD pair to its least-cost route by MSA.

Step 1.4. Repeat Step 1.3 until an equilibrium is reached. Under the equilibrium, derive the route-based OD matrices, $\{\lambda_{o,d}^I\}$, where $\lambda_{o,d}^I$ represents the demand of OD pair (o, d) that choose route $I \in \{t, bt, tb, btb, b\}$. Record the boarding/alighting demand variables for each bike station $m \in \{1,2, \dots, n_b\}$ and each transit stop $j \in \{1,2, \dots, n_t\}$, including $\{b_m^I, a_m^I\}$, $\{B_{m,b}, A_{m,b}\}$, and $\{B_{j,t}, A_{j,t}\}$, using equations similar to (6-11).

Step 2. System cost calculation.

Step 2.1. Compute patrons' cost items.

(i) The total access and egress time to and from bike stations and transit stops is calculated by $\tilde{C}_a = \sum_{m=1}^{n_b} \left(\sum_{I \in \{t,tb\}} \left(b_m^I \frac{H_m^{j_m} d_m^{j_m}}{v_w} \right) + \sum_{I \in \{t,bt\}} \left(a_m^I \frac{H_m^{j_m} d_m^{j_m}}{v_w} \right) \right) + \sum_{m=1}^{n_b} \left(\left(1 - H_m^{j_m}\right) \left(\sum_{I \in \{bt,btb\}} \left(b_m^I \frac{d_m^{j_m}}{v_b} \right) + \sum_{I \in \{tb,btb\}} \left(a_m^I \frac{d_m^{j_m}}{v_b} \right) \right) \right) + \tilde{c}_a$, where the first term on the right-hand side (RHS) is the able-bodied patrons' walking time to and from transit stops; the second term is the able-bodied patrons' cycling time to and from transit stops; and the third term $\tilde{c}_a$ denotes the sum of the able-bodied patrons' walking time to and from bike stations and the non-able-bodied ones' walking time to and from transit stops. The last term does not depend on the route assignment and is given by

$$\tilde{c}_a = \beta \sum_{m=1}^{n_b} \left(\int_{l_m^b}^{r_m^b} \frac{\left(\int_{u=x}^{L} \lambda(x,u) du + \int_{u=0}^{x} \lambda(u,x) du \right) x}{v_w} dx \right) + (1 - \beta) \sum_{j=1}^{n_t} \left(\int_{l_j^t}^{r_j^t} \frac{\left(\int_{u=x}^{L} \lambda(x,u) du + \int_{u=0}^{x} \lambda(u,x) du \right) x}{v_w} dx \right).$$

(ii) Wait time at transit stops and pick-up and drop-off delays at bike stations: $\tilde{C}_w = \frac{h}{2}\sum_{j=1}^{n_t} B_{j,t} + \sum_{m=1}^{n_m}\left(t_{pu}B_{m,b} + t_{do}A_{m,b}\right)$, where $B_{j,t}$, $B_{m,b}$ and $A_{m,b}$ are obtained in Step 1.

(iii) Riding time in transit vehicles and on bikes: $\tilde{C}_v = \sum_{j=1}^{n_t} o_{j,t}\left(\frac{\left(x_{j+1}^t - x_j^t\right)}{v_t} + \left(\tau^0 + h \cdot \max\left(\tau^b B_{j,t}, \tau^a A_{j,t}\right)\right)\right) + \sum_{m=1}^{n_b}\frac{x_{m+1}^b - x_m^b}{v_b}\sum_{u=1}^{m}\left(b_u^b - a_u^b\right)$, where the cross-sectional transit flow at transit stop j is obtained by $o_{j,t} = \sum_{u=1}^{j}\left(B_{u,t} - A_{u,t}\right)$.

(iv) Transfer time: $\tilde{C}_f = \xi\sum_{m=1}^{n_b}\left(1 - H_m^{j_m}\right)\left(\sum_{I\in\{tb,btb\}} a_m^I + \sum_{I\in\{bt,btb\}} b_m^I\right)$, where a_m^I and b_m^I are obtained in Step 1.

Step 2.2. Compute agency cost items. Calculate the transit and bike-sharing agency costs, $\tilde{C}_t^O$ and $\tilde{C}_b^O$, using the model presented in Section 3.4. The calculation will use the following variables:

(i) Transit line length: $L = \left(x_{n_t}^t - x_1^t\right)$. Note that this may be shorter than the corridor length since the first and last transit stops are not necessarily located at the very ends of the corridor.

(ii) Vehicle-hours traveled per operation hour: $\frac{1}{h}\sum_{j=1}^{n_t}\left(\frac{\left(x_{j+1}^t - x_j^t\right)}{v_t} + \left(\tau^0 + h \cdot \max\left(\tau^b B_{j,t}, \tau^a A_{j,t}\right)\right)\right)$ for transit vehicles; and $\sum_{m=1}^{n_b}\left(\frac{o_{m,b}}{v_b} + t_{pu}B_{m,b} + t_{do}A_{m,b}\right)$ for shared bikes, where the cross-sectional bike-riding flow is obtained by $o_{m,b} = \sum_{u=1}^{m}\left(B_{u,b} - A_{u,b}\right)$.

(iii) Re-estimate the bike rebalancing cost using the method proposed in Appendix C.

Step 2.3. Calculate the generalized cost as $\tilde{Z} = \left(\tilde{C}_a + \tilde{C}_w + \tilde{C}_v + \tilde{C}_f\right) + \frac{1}{\mu}\left(\tilde{C}_t^O + \tilde{C}_b^O\right)$.

Appendix F: Effects of $\mathcal{M}$ on the solution quality and computation times

Table F1. Solution quality and computation time for different $\mathcal{M}$'s.

$\mathcal{M}$	100	200	300	400	500
Average percentage error of generalized cost against $\mathcal{M} = 500$	0.69%	0.26%	0.11%	0.04%	-
Maximum percentage error of generalized cost against $\mathcal{M} = 500$	0.88%	0.32%	0.17%	0.06%	-
Average CPU time (s)	9.1	31.4	73.3	152.7	232.8
Maximum CPU time (s)	9.6	33.1	75.5	155.4	236.7

The second and third rows of Table F1 summarize the average and maximum errors created by the discretization method. The errors were calculated by comparing the generalized costs of $\mathcal{M} \in \{100,200,300,400\}$ (meaning that $\Delta x \in \{200,100,67,50,40\}$ m) against that of $\mathcal{M} = 500$ (meaning that $\Delta x = 40$ m). Although we do not have the limiting cost value when $\mathcal{M} \to \infty$, we believe that the case of $\mathcal{M} = 500$ is accurate enough to serve as a benchmark. The tabulated values were calculated for

the 90 numerical instances used in Section 5.2. They show that even using a large discretization interval of $\Delta x = 200$ m brings only a cost error of less than 1%. This result speaks to the accuracy of our method of discretization.

The fourth and fifth rows of Table F1 present the average and maximum CPU times for the 90 instances examined with each of the five values of $\mathcal{M}$. These results were obtained using Matlab R2018a on a PC with a Windows 10 64-bit OS, 16G RAM, and an Intel Xeon E5-2450 2.1GHz CPU. The values show that the runtimes increase rapidly with $\mathcal{M}$ (as expected). However, even with a large value of $\mathcal{M} = 500$, a solution can be obtained within 4 minutes for all the instances tested. Our choice of $\mathcal{M} = 400$ in Section 5 reflects a good tradeoff between computational efficiency and solution quality.

References

Badia, H., Estrada, M., Robusté, F., 2014. Competitive transit network design in cities with radial street patterns. Transportation Research Part B 59, 161-181.

Badia, H., 2020. Comparison of bus network structures in face of urban dispersion for a ring-radial city. Networks and Spatial Economics 20, 233-271.

Bike to everything, 2019. https://biketoeverything.com/2019/01/04/electric-scooter-vs-electric-bicycle-thoughts-on-the-new-electric-scooter-share/

Call a bike, 2019. https://www.callabike-interaktiv.de/en/cities/Berlin

Campbell, K.B., Brakewood, C., 2017. Sharing riders: How bikesharing impacts bus ridership in New York City. Transportation Research Part A 100, 264-282.

Ceder, A., Butcher, M., Wang, L., 2015. Optimization of bus stop placement for routes on uneven topography. Transportation Research Part B 74, 40-61.

Chen, H., Gu, W., Cassidy, M.J., Daganzo, C.F., 2015. Optimal transit service atop ring-radial and grid street networks: A continuum approximation design method and comparisons. Transportation Research Part B 81, 755-774. https://doi.org/10.1016/j.trb.2015.06.012

Chen, J., Liu, Z., Wang, S., Chen, X., 2018. Continuum approximation modeling of transit network design considering local route service and short-turn strategy. Transportation Research Part E 119, 165-188.

Chen, P., Nie, Y.M., 2017. Connecting e-hailing to mass transit platform: Analysis of relative spatial position. Transportation Research Part C 77, 444-461. https://doi.org/10.1016/j.trc.2017.02.013

Chow, J.Y.J., Sayarshad, H.R., 2014. Symbiotic network design strategies in the presence of coexisting transportation networks. Transportation Research Part B, 13-34. https://doi.org/10.1016/j.trb.2014.01.008

Conrow, L., Murray, A.T., Fischer, H.A., 2018. An optimization approach for equitable bicycle share station siting. Journal of Transport Geography 69, 163-170.

Freund, D., Henderson, S. G., Shmoys, D.B., 2017. Minimizing multimodular functions and allocating capacity in bike-sharing systems, in: International Conference on Integer Programming and Combinatorial Optimization. Springer.

Daganzo, C.F., 2010. Structure of competitive transit networks. Transportation Research Part B 44, 434-446. https://doi.org/10.1016/j.trb.2009.11.001

Estrada, M., Roca-Riu, M., Badia, H., Robusté, F., Daganzo, C.F., 2011. Design and implementation of efficient transit networks: Procedure, case study and validity test. Procedia - Social and Behavioral Sciences 17, 113-135. https://doi.org/10.1016/j.sbspro.2011.04.510

Fan, W., Mei, Y., Gu, W., 2018. Optimal design of intersecting bimodal transit networks in a grid city. Transportation Research Part B 111, 203–226. https://doi.org/10.1016/j.trb.2018.03.007.

Gauthier, A., Hughes, C., Kost, C., Li, S., Linke, C., Lotshaw, S., Mason, J., Pardo, C., Rasore, C., Bradley, S., Trevino, X., 2013. The Bike-Share Planning Guide. Institute for Transportation and Development Policy, New York, NY.

García-Palomares, J.C., Gutiérrez, J., Latorre, M., 2012. Optimizing the location of stations in bike-sharing programs: A GIS approach. Applied Geography 35, 235-246.

Gleason, R., Miskimins, L., 2012. Exploring Bicycle Options for federal Lands: Bike Sharing, Rentals and Employee Fleets. Publication FHWA-WFL/TD-12-001. FHWA, U.S. Department of Transportation.

Graehler Jr., M., Mucci, R.A., Erhardt, G.D., 2019. Understanding the recent transit ridership decline in major us cities: service cuts or emerging modes? Transportation Research Board 98th Annual Meeting, Washington DC.

Gu, W., Amini, Z., & Cassidy, M. J., 2016. Exploring alternative service schemes for busy transit corridors. Transportation Research Part B 93, 126-145.

Li X., Luo, Y., Wang, T., Jia, P., Kuang, H., 2020. An integrated approach for optimizing bi-modal transit networks fed by shared bikes. Transportation Research Part E 141, 102016.

Lin, J.R., Yang, T.H., Chang, Y.C., 2013. A hub location inventory model for bicycle sharing system design: Formulation and solution. Computers & Industrial Engineering 65, 77-86.

Lin, J.R., Yang, T.H., 2011. Strategic design of public bicycle sharing systems with service level constraints. Transportation Research Part E 47, 284-294. https://doi.org/10.1016/j.tre.2010.09.004

Liu, L., Sun, L., Chen, Y., Ma, X., 2019. Optimizing fleet size and scheduling of feeder transit services considering the influence of bike-sharing systems. Journal of Cleaner Production 236, 117550.

Luo, S., Nie, Y.M., 2019. Paired-line hybrid transit system in a monocentric city with exponential demand pattern. Transportation Research Record 1-13.

Luo, S., Nie, Y.M., 2020a. Paired-line hybrid transit design considering spatial heterogeneity. Transportation Research Part B 132, 320-339.

Luo, S., Nie, Y.M., 2020b. On the role of route choice modeling in transit sketchy design. Transportation Research Part A 136, 223-243.

Luo, X., Fan, W., Jiang, Y., Zhang, J., 2020. Optimal design of bus stop locations integrating continuum approximation and discrete models. Journal of Advanced Transportation 2020, 8872748.

Ma, T., Liu, C., Erdoğan, S., 2015. Bicycle sharing and public transit: Does capital bikeshare affect metrorail ridership in Washington, D.C.? Transportation Research Record 2534, 1-9.

Ma, X., Zhang, X., Li, X., Wang, X., Zhao, X., 2019. Impacts of free-floating bikesharing system on public transit ridership. Transportation Research Part D 76, 100-110.

Martens, K., 2004. The bicycle as a feedering mode: Experiences from three European countries. Transportation Research Part D 9, 281-294. https://doi.org/10.1016/j.trd.2004.02.005

MathWorks, 2019. https://www.mathworks.com/matlabcentral/fileexchange/8998-surface-fittingusing-gridfit.

Mei, Y., Gu, W., Cassidy, M, Fan, W., 2021. Planning skip-stop transit service under heterogeneous demands. To appear in Transportation Research Part B. https://arxiv.org/abs/2011.12674

Metro Bike share, 2019. https://bikeshare.metro.net/

Medina, M., Giesen, R., Muñoz, J.C., 2013. Model for the optimal location of bus stops and its application to a public transport corridor in Santiago, Chile. Transportation Research Record 2352, 84-93. https://doi.org/10.3141/2352-10

Murray, A.T., 2003. A coverage model for improving public transit system. Annals of Operations Research 123, 143-156. https://doi.org/10.1023/A:1026123329433

Nair, R., Miller-Hooks, E., 2011. Fleet management for vehicle sharing operations. Transportation Science 45, 524-540. https://doi.org/10.1287/trsc.1100.0347

National Association of City Transportation Officials (NACTO),2018. https://nacto.org/shared-micromobility-2018/

Nayeem, M. A., Rahman, M. K., Rahman, M. S. 2014. Transit network design by genetic algorithm with elitism. Transportation Research Part C, 46, 30-45.

Newell, G.F., 1971. dispatching policies for a transportation route. Transportation Science 5, 91-105.

Ouyang, Y., Daganzo, C.F., 2006. Discretization and validation of the continuum approximation scheme for terminal system design. Transportation Science 40(1), 89-98.

Ouyang, Y., Nourbakhsh, S.M., Cassidy, M.J., 2014. Continuum approximation approach to bus network design under spatially heterogeneous demand. Transportation Research Part B 68, 333-344. https://doi.org/10.1016/j.trb.2014.05.018

Pal, A., Zhang, Y., 2017. Free-floating bike sharing: Solving real-life large-scale static rebalancing problems. Transportation Research Part C 80, 92-116. https://doi.org/10.1016/j.trc.2017.03.016

Parkes, S.D., Marsden, G., Shaheen, S.A., Cohen, A.P., 2013. Understanding the diffusion of public bikesharing systems: Evidence from Europe and North America. Journal of Transport Geography 31, 94-103. https://doi.org/10.1016/j.jtrangeo.2013.06.003

People's daily, 2018. http://en.people.cn/n3/2018/0208/c90000-9425354.html

Rietveld, P., 2000. The accessibility of railway stations: The role of the bicycle in The Netherlands. Transportation Research Part D 5, 71-75. https://doi.org/10.1016/S1361-9209(99)00019-X

Shaheen, S., Guzman, S., Zhang, H., 2010. Bikesharing in Europe, the Americas, and Asia. Transportation research record 2143,159-167. https://doi.org/10.3141/2143-20

Sheffi, Y., 1985. Urban Transportation Networks: Equilibrium Analysis with Mathematical Programming Methods. Prentice-Hall, Inc., New Jersey.

Shu, J., Chou, M.C., Liu, Q., Teo, C.P., Wang, I.L., 2013. Models for effective deployment and redistribution of bicycles within public bicycle-sharing systems. Operations Research 61, 1346-1359. https://doi.org/10.1287/opre.2013.1215

Sivakumaran, K., Li, Y., Cassidy, M., Madanat, S., 2014. Access and the choice of transit technology. Transportation Research Part A 59, 204-221. https://doi.org/10.1016/j.tra.2013.09.006

Singleton, P.A., Clifton, K.J., 2014. Exploring synergy in bicycle and transit use: Empirical evidence at two scales. Transporation research record 2417, 92-102. https://doi.org/10.3141/2417-10

Sun, J., 2017. Accessing Public Transit by Bike Sharing System. Cornell University.

Szeto, W. Y., Wu, Y. 2011. A simultaneous bus route design and frequency setting problem for Tin Shui Wai, Hong Kong. European Journal of Operational Research, 209(2), 141-155.

Tang, G., Keshav, S., Golab, L., Wu, K., 2018. Bikeshare pool sizing for bike-and-ride multimodal transit. IEEE Transactions on Intelligent Transportation 19, 2279-2289.

Tang, Y., Pan, H., Shen, Q., 2011. Bike-sharing systems in Beijing, Shanghai, and Hangzhou and their impact on travel behavior. Transportation Research Board 90th Annual Meeting, Washington DC.

Tavassoli, K., Tamannaei, M., 2020. Hub network design for integrated bike-and-ride services: A competitive approach to reducing automobile dependence. Journal of Cleaner Production 248, 119247. https://doi.org/10.1016/j.jclepro.2019.119247

Vaughan, R.J，Cousins, E.., 1977. Optimum location of stops on a bus route, in: Proceedings of 7th International Symposium of Transportation and Traffic Theory. Kyoto. 697-719.

Wikipedia, 2019. Bike-sharing system. https://en.wikipedia.org/wiki/Bicycle-sharing_system

Wirasinghe, S.C., Ghoneim, N.S., 1981. Spacing of bus-stops for many to many travel demand. Transportation Science 15, 210-221. https://doi.org/10.1287/trsc.15.3.210

Wu, L., Gu, W., Fan, W., Cassidy, M.J., 2020. Optimal design of transit networks fed by shared bikes. Transportation Research Part B 131, 63-83. https://doi.org/10.1016/j.trb.2019.11.003

Yang, M., Liu, X., Wang, W., Li, Z., Zhao, J., 2016. Empirical analysis of a mode shift to using public bicycles to access the suburban metro: Survey of Nanjing, China. Journal of Urban Planning & Development 142 05015011//doi.org/10.1061/(ASCE)UP.1943-5444.0000299